University of Szeged

Faculty of Pharmacy

Institute of Pharmacognosy

PREPARATION OF BIOACTIVE OXIDIZED HYDROXYCINNAMIC ACID DERIVATIVES

Ph.D. Thesis

Laura Fási, Pharm.D.

Supervisor:

Attila Hunyadi, Ph.D.

Institute of Pharmacognosy
University of Szeged, Szeged, Hungary

Co-supervisor:

Fang-Rong Chang, Ph.D.

Graduate Institute of Natural Products
Kaohsiung Medical University, Kaohsiung, Taiwan

Szeged, Hungary

2021

Table of contents

LIST OF PUBLICATIONS RELATED TO THE THESIS

I. **Fási L**, Di Meo F, Kuo C-Y, Stojkovic Buric S, Martins A, Kúsz N, Béni Z, Dékány M, Balogh GT, Pesic M, Wang H-C, Trouillas P, Hunyadi A, Antioxidant-inspired drug discovery: antitumor metabolite is formed in situ from a hydroxycinnamic acid derivative upon free-radical scavenging, *Journal of Medicinal Chemistry* 2019, 62, 3, 1657-1668.

IF: 6.205

Drug discovery: **D1** (2019)

II. **Fási L**, Latif AD, Zupkó I, Lévai S, Dékány M, Béni Z, Könczöl Á, Balogh GT, Hunyadi A, AAPH or peroxynitrite-induced biorelevant oxidation of methyl caffeate yields potent antitumor metabolite, *Biomolecules* 2020, 10, 1537.

IF: 4.082

Biochemistry: **Q1** (2019-2020)

LIST OF ABBREVIATIONS

1D	One-dimensional
2D	Two-dimensional
^{1}H NMR	Proton nuclear magnetic resonance spectroscopy
^{13}C NMR	Carbon nuclear magnetic resonance spectroscopy
AAPH	2,2′- azobis(2-methylpropionamidine) dihydrochloride
ABTS	2,2′- azino-bis(3-ethylbenzothiazoline-6-sulfonic acid)
anhydr.	Anhydrous
aq.	Aqueous
ATM	Ataxia telangiectasia mutated kinase
ATR	Ataxia telangiectasia and Rad3-related kinase
BDE	Bond dissociation enthalpy
BHT	Butylated hydroxytoluene
CAPE	Caffeic acid phenethyl ester
CFR	Continuous flow reaction
CI	Combination index
CID	Collision induced dissociation
conc.	Concentrated
COX-2	Cyclooxygenase-2
DDR	DNA damage responses
DFT	Density functional theory
DHE	Dihydroethidium
DMSO	Dimethyl sulfoxide
DPPH	2,2-Diphenyl-1-picrylhydrazyl
DSB	Double strand break
EC_{50}	Half maximal effective concentration
ECL	Enhanced chemiluminescence
ESI	Electron spray ionization
FBS	Fetal bovine serum
FRAP	Fluorescence recovery after photobleaching
GI_{50}	Half maximum growth inhibitory concentration
HAT	Hydrogen-atom transfer
HCAs	Hydroxycinnamic acids

HPLC	High-performance liquid chromatography
HRP	Horseradish peroxidase
IC_{50}	Fifty percent inhibitory concentration
MDR	Multiple drug resistance
MIC	Minimum inhibitory concentration
MTT	3-(4,5-dimethylthiazol-2-yl)-2,5-diphenyltetrazolium bromide
NF-κB	Nuclear factor kappa beta
PBS	Phosphate-buffered saline
PCC	Pyridinium chlorochromate
PIDA	(Diacetoxyiodo)benzene
PIFA	[Bis(trifluoroacetoxy)iodo]benzene
RNS	Reactive nitrogen species
ROS	Reactive oxygen species
RP-HPLC	Reversed-phase high performance liquid chromatography
SAR	Structure-activity relationship
SEM	Standard error of the mean
SET	Single-electron transfer
SFC	Supercritical fluid chromatography
SOD	Superoxide dismutase
t-BHP	*tert*-butyl hydroperoxide
TBA	Thiobarbituric acid
TCA	Trichloroacetic acid
TFA	Trifluoroacetic acid
TLC	Thin-layer chromatography
TNF	Tumor necrosis factor
UV	Ultraviolet

1. INTRODUCTION

1.1 Cinnamic acids – occurrence and chemical characterization

Phenolic acids are among the most abundant secondary plant metabolites, and they are widely recognized as dietary antioxidants [1]. Cinnamic acids and benzoic acids represent the two major groups of phenolic acids that occur in nature mainly as hydroxybenzoic and hydroxycinnamic acids (HCAs) [2]–[4]. HCAs are ubiquitous in dietary plants, and they are present in grains (*e.g.*, brans, whole wheat and corn flour, white wheat bread), fruits (*e.g.*, apples, plums, berries, cherries, peaches, grapes, citrus fruits), vegetables (*e.g.*, carrot, cabbage, eggplant, potato, broccoli, lettuces), spices (*e.g.*, basil, pepper), nuts (*e.g.*, peanut), dark chocolate and in beverages (*e.g.*, coffee, tea, beer, wine) [5].

The basic skeleton of HCAs consists of nine carbon atoms (C6C3), forming a phenylpropanoid structure [5]. The most common HCAs are *p*-coumaric, caffeic, ferulic and sinapic acids, and occur in nature in their free forms or esters formed with quinic acid or glucose, or they can form more complex derivatives such as dimers, trimers, etc. [6], [7]. A general structural formula of HCAs is represented in Figure 1. HCAs and other phenolic compounds such as lignans, coumarins, lignins, anthocyanins are biosynthesized via the shikimate pathway, in that the amino acid phenylalanine is an important intermediate product [8].

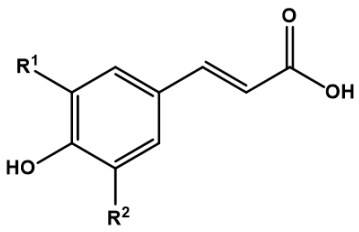

	R^1	R^2
p-coumaric acid:	-	-
caffeic acid:	OH	-
ferulic acid:	OMe	-
sinapic acid:	OMe	OMe

Figure 1. Chemical structure of the most abundant natural HCAs.

1.2 Semi-synthetic transformations, oxidations of hydroxycinnamic acids

Antioxidants attracted a tremendous scientific interest in the past few decades due to their multiple alleged health benefits in a wide variety of chronic diseases, and their abundance in dietary plants [9]–[11]. It is well known that antioxidants can scavenge reactive oxygen and nitrogen species (ROS and RNS), which may counteract the harmful effects of such species on biological systems [12]. From such an interaction, however, possible bioactive metabolites of the antioxidants may also be formed [13]. Biomimetic oxidative chemical reactions can be considered as relevant models of ROS or RNS scavenging, and therefore they provide a valuable toolkit to explore such metabolites through diversity-oriented synthesis [13].

In 1995, J.J. Bozell *et al*. found that para-substituted phenolics can be oxidized to the corresponding benzoquinone in the presence of oxygen and Co-Schiff base complex as catalyst [14]. According to a previous publication, in which the oxidation of various polyphenols with oxygen in the presence of a catalytic amount of Fe^{3+} ions was described, caffeic acid, sinapic acid, chlorogenic acid and rosmarinic acid (along with other acids) were completely oxidized in 10 days, and led to complex metabolite fingerprints [15]. Another example for the biomimetic transformation of cinnamic acid derivatives (*p*-coumaric, caffeic and ferulic acid methyl esters), is their oxidation in a mixture of anhydr. benzene and anhydr. acetone with the addition of silver oxide (Ag_2O) as catalyst, generating dihydrobenzofuran lignans with potent antitumor activities [16].

Previously, our research group reported the simple and quick semi-synthesis of a protoflavonoid, protoapigenone from a 4′-hydroxyflavone, apigenin, using a hypervalent iodine reagent, [bis(trifluoroacetoxy)iodo]benzene (PIFA) [17]. PIFA can oxidize phenolic compounds through single-electron transfer (SET) whose intermediate can go through deprotonation and form the same phenoxyl radical that is formed in a hydrogen-atom transfer (HAT) reaction [13]. Therefore, in some circumstances, this reagent may also be considered as "biomimetic-like", and its use may lead to the formation of metabolites like those that are formed upon free-radical scavenging.

The metabolites arising from ROS or RNS scavenging by antioxidants may have largely different, and in some cases much stronger bioactivities when compared to their parent compounds [13]. Due to their simple chemical structure and abundance in dietary plants, HCAs are ideal candidates to initiate related studies. Accordingly, this PhD work aimed to evaluate free radical scavenging-mediated formation of hydroxycinnamic acid metabolites by using a variety of oxidative chemical approaches, and to find bioactive compounds among these metabolites.

1.3 Bioactivity of cinnamic acids and derivatives, structure-activity relationships

Antioxidant effect

Based on the central role of oxidative stress in the rise and progress of pathological conditions such as cancer, cardiovascular and neurodegenerative diseases, type II diabetes, etc. [7], the antioxidant effect of natural compounds is of importance for drug discovery. Phenolic compounds are strong antioxidants as they can act as hydrogen donors and reducing agents, and they can quench singlet oxygen and chelate metal ions [18]. Caffeic, sinapic and ferulic acids have stronger reducing power than butylated hydroxytoluene (BHT), and comparable to that of

Trolox [19]. The structural elements of HCAs that are important in terms of antioxidant effect are the followings. Hydroxy functions on the benzene ring can produce a highly resonance stabilized phenoxyl radical intermediate through delocalization of the unpaired electron; the extended conjugation provided by the unsaturated sidechain greatly contributes to this [20]. The number of the hydroxy groups on the aromatic ring of HCAs can influence the antioxidant activity [7]. When compared to a monohydroxy compound (*e.g.*, *p*-coumaric acid), a dihydroxy derivative (*e.g.*, caffeic acid) has higher singlet oxygen quenching [21], and hypochlorite scavenging activities [22], and it can efficiently block LDL peroxidation [7], [23]. In ABTS and DPPH assays, trihydroxylated phenols (pyrogallol moiety) showed better antioxidant activity than the dihydroxylated caffeic acid (catechol moiety). However, due to their higher lipophilicity, dihydroxylated cinnamic acids proved to be more potent antioxidants in biological systems than the trihydroxylated ones [24]. The presence of a catechol moiety can increase the antiradical activity due to the stabilization of intramolecular H-bonds [7], [18]. A number of publications point out that compounds bearing a catechol moiety such as caffeic acid have the strongest antioxidant properties in various assays (*e.g.*, DPPH, lipid autooxidation, superoxide dismutase (SOD) activity, catalase activity, glutathione peroxidase activity) [25], [26]. Concerning the role of methoxy groups, the antioxidant activity of cinnamic acids follows the order of *p*-coumaric acid < ferulic acid < sinapic acid, and this can be explained by the electron-donating property of the methoxy group that can also stabilize the phenoxy radical [27]. Nevertheless, caffeic acid is a stronger antioxidant than ferulic acid [28]. Esterification of the side chain increases the lipophilicity of HCAs, hence improving their antioxidant properties in lipophilic systems, but most of the esterified HCAs are weaker reducing agents than the free acids according to results obtained by FRAP assays [29]–[31]. Concerning ester groups, caffeic acid esters (*e.g.*, ethyl ester, chlorogenic acid, rosmarinic acid) can produce a more stable *o*-quinone form as compared to the unesterified HCAs that can yield an unstable phenoxy radical upon oxidation [32]. HCAs with a catechol moiety also have the chelation ability with transition metal ions such as Fe(II), Fe(III), Cu(II), therefore repressing Fenton reactions that would produce highly toxic radicals such as hydroxyl radical from hydrogen peroxide [33].

Antitumor effect

Extensive studies are available on the antitumor potential of cinnamic acid derivatives including HCAs. Ekmekcioglu *et al*. revealed that cinnamic acid (2.5-8.0 mM) is an antiproliferative agent and inhibits the DNA synthesis on growing cells in human colon adenocarcinoma cells (Caco-2) [34]. In another study, cinnamic acid was reported to reduce

cell proliferation in glioblastoma, melanoma, prostate and lung carcinoma cells with the IC_{50} values of 1-4.5 mM [35]. This efficacy is rather low. Caffeic acid showed no detectable cytotoxic activity at up to 40 μM concentration *in vitro* against acute myeloid leukemia (HL-60) cells as published by Nitzsche *et al*. [36]. On the other hand, caffeic acid was able to suppress UVB-induced skin carcinogenesis through the inhibition of Fyn kinase, a non-receptor protein tyrosine kinase, which was found to be required for UVB-induced cyclooxygenase-2 (COX-2) expression [37], [38].

The ester derivatives of HCAs have much stronger antitumor effect than their free acid counterparts. For example, two components of propolis, phenethyl caffeate (CAPE) and cinnamyl caffeate had potent antiproliferative activity against murine colon 26-L5 carcinoma with half maximal effective concentration (EC_{50}) values of 1.76 μM and 0.11 μM, respectively [39]. Natarajan *et al*. found that CAPE inhibited nuclear factor kappa beta (NF-κB) activation induced by the inflammatory agent tumour necrosis factor (TNF) and agents producing ROS [40]. NF-κB protects cancer cells from apoptosis and increasing their growth activity in cholangiocarcinoma cells [38]. Methyl caffeate was reported to exert cytotoxic effect with IC_{50} values of around 10 μM against various cancer cell lines such as murine melanoma (B16), human colon cancer (HCT116), human epidermoid carcinoma (A431) [41]. There are some conflicting results on the efficacy of methyl caffeate against MCF-7 human breast cancer cell line cells. In one study, it was found to have *in vitro* antiproliferative activity with an IC_{50} value of ca. 110 μM [42], while in another study much stronger antitumor effect was found with an IC_{50} value of 0.62 μM on cell viability and the induction of apoptotic cell death in MCF-7 cells [43] [13].

In the above-mentioned Ag_2O-catalysed biomimetic oxidation of cinnamic acid esters, a set of dihydrobenzofuran lignans were prepared with highly potent antitumor activity. The oxidized dimer of methyl caffeate showed particularly strong antiproliferative activity with half maximum growth inhibitory concentrations (GI_{50}) lower than 10 nM against breast cancer cell lines (MDA-MB-435, MDA-N and BT-549) [16]. Furthermore, it was shown that the 2*R*,3*R* enantiomer of that dimer is a potent antitubulin agent (IC_{50} = 6.0 μM) [16]. The antiangiogenic activity of this compound (especially the 2*R*,3*R*) was described by Apers *et al*. [44], and similar activity was reported for the dihydrobenzofuran neolignan derivative of methyl ferulate on angiogenesis [45]. In a recent study, Yin *et al*. reported about a significant antimetastatic activity of the dimer of methyl caffeate on mammary tumours; this compound exerted its activity on the microenvironment of the tumour by the induction of IL-25 secretion from tumour-associated fibroblasts at concentrations of 20-100 μg kg^{-1} body weight in mice [46].

Antimicrobial effect, antiviral effect

Ferulic, *p*-coumaric and sinapic acid showed antibacterial activity (mean MIC 3.0 mM) against several Gram-negative bacteria (e.g. *Escherichia coli*) [47]. Another widespread HCA derivative, rosmarinic acid is also known for its antibacterial effect against several bacteria, such as *Bacillus subtilis*, *Escherichia coli*, *Micrococcus luteus* [48]. Tonari *et al*. investigated the antibacterial activity of cinnamic acid derivatives in correlation with their structures. According to their results, compounds having substituted phenyl group showed the strongest antibacterial activity against *B. subtilis* and *E. coli* [49].

Further, several HCAs were also found to have antiviral effect. Rosmarinic acid and its methyl ester were reported to have inhibitory activity against HIV-1 integrase, an essential enzyme for the replication of HIV that mediates the viral genome integration into the host cells chromosomes [50]. Several semi-synthetic and synthetic cinnamic acid derivatives showed promising results in antiviral experiments against viruses such as HIV, influenza, rhinoviruses, herpes simplex virus type 2, etc. [18].

2. OBJECTIVES

The aim of this Ph.D. work was to study HCA metabolites that may form through ROS/RNS scavenging by these compounds. This work was initiated as the beginning of an antioxidant-inspired drug discovery program to identify new bioactive compounds from the diversity-oriented transformation of antioxidants through biomimetic oxidative chemistry. Accordingly, the following objectives were set up for the Ph.D. work presented in this dissertation:

1. **Preparation of semi-synthetic oxidized hydroxycinnamic acid derivatives.** Different kinds of biomimetic or bio-inspired oxidative reagents were selected, including hypervalent iodine compounds (PIFA, PIDA), peroxynitrite and AAPH, to investigate the formation of HCA metabolites. Further *p*-quinol and *O*-alkyl analogues were prepared to evaluate structure-activity relationships. Purification of the oxidized metabolites was carried out by combined chromatographic techniques.
2. **Biological evaluation of the isolated oxidized hydroxycinnamic acid derivatives.** Bioactivity testing of the purified oxidized metabolites in comparison with their parent compounds was planned in research cooperation.
3. **Investigation of the formation of hydroxycinnamic acid metabolites in biorelevant environment.** The possible formation of the identified metabolites upon free radical

scavenging by HCAs was studied by various *in vitro* and *in silico* techniques, to evaluate the chance of their formation in a biological environment under oxidative stress.

3. MATERIALS AND METHODS

3.1 Chromatography

High-performance liquid chromatography (HPLC):

HPLC1: Analytical high-performance liquid chromatography was performed on a gradient system of two pumps (PU-2080) connected to a photodiode-array detector (MD-2010) (Jasco Analytical Instruments, Tokyo, Japan).

HPLC2: Semi-preparative HPLC purification was carried out on a system of two Waters 600 pumps connected to a Waters 600 2λ detector (Waters, Milford, Massachusetts, USA), on a Kinetex XB-C18 (5 μm, 100 Å, AX, 250x21.2 mm) column.

HPLC3: Analytical high-performance liquid chromatography and semi-preparative purification was performed on a system, included a binary pump (LC-20AD) and a diode array detector (SPD-M10A VP) (Shimadzu, Kyoto, Japan).

HPLC4: Purification was performed on a Shimadzu LC-8 preparative HPLC, on a gradient system of two preparative pumps (LC-8A) connected to a diode array detector (SPD M20A). Additional parts of the HPLC system: autosampler (SIL-10AP), fraction collector (FRC-10A), communications bus module (CMB-20A), column oven (CTO-20AC).

HPLC5: Preparative HPLC was performed by using the pump, detector and fraction collector of an Armen Spot CPC (Armen Instrument, Saint Ave, France).

LC-DAD-MS analysis was carried out on an Agilent 1200 liquid chromatography system coupled with a triple quadrupole mass spectrometer (Agilent 6410) equipped with an ESI source (Agilent Technology, Waldbronn, Germany).

Flash chromatography was performed on a CombiFlash Rf+ equipment (Teledyne ISCO, USA).

Supercritical fluid chromatography (SFC) was performed on a Jasco semi-preparative chromatographic system (PU-4386 and PU-4086 pumps, AS-4350 SFC autosampler, CO4060 column oven, BP-4340 back-pressure regulator; Jasco Analytical Instruments, Tokyo, Japan), on a Luna Silica (2) column (5 μm, 100 Å, 250x4.6 mm, Phenomenex, Torrance, CA, USA), with the solvent system CO_2 – EtOH (9:1, v/v), at the temperature of 30 °C, at the pressure of 25 MPa, and at the flow rate of 2 mL/min.

The most frequently used solvent system:

Solvent system 1: a gradient elution of acetonitrile from 30 to 70 % in water at 0-12 min, 70 % of acetonitrile at 12-14 min, from 14.01 back to 30 % of acetonitrile, total running time 25 min.

3.2 Starting materials and reagents

3.2.1 Cinnamic acids and reagents

Caffeic acid, *p*-coumaric acid, methyl *p*-coumarate, AAPH and the hypervalent iodine reagents Bis[trifluoroacetoxy)iodo]benzene (PIFA) and (Diacetoxyiodo)benzene (PIDA) were purchased from Sigma Aldrich (Munich, Germany). Analytical and HPLC-grade solvents were purchased from Molar Chemicals (Halásztelek, Hungary).

3.2.2 Preparation of cinnamic acid esters as starting materials

p-Coumarate esters (**1**-**4**) were prepared by Fischer esterification. An aliquot of 1.66 mmol of *p*-coumaric acid was dissolved in 100 ml of the esterifying alcohol (methanol, ethanol, butanol, isopropyl-alcohol) that was previously made anhydrous by molecular sieve (0.3 nm). The solution was stirred under reflux, and 2 ml of conc. H_2SO_4 was added. The reaction was monitored by thin-layer chromatography (TLC), and when the starting material was not detectable anymore, the reaction mixture was cooled down to room temperature, neutralized with the addition of $NaHCO_3$ solution, and evaporated under reduced pressure. Liquid-liquid extraction between water and 5x50 ml of dichloromethane was used to extract esters, and the organic phase was dried with anhydrous Na_2SO_4. Finally, the solution was dried under vacuum, and the ester was crystallized [45]. In the case of methyl *p*-coumarate (**4**), commercially obtained compound was also used in this work.

To prepare methyl caffeate (**5**), 1.0 g of caffeic acid was dissolved in 12 ml of anhydrous methanol. The solution was stirred under reflux, and when the temperature reached 60 °C, 0.1 g of Dowex 50 W cation exchange resin (Sigma, St. Louis, MO, USA) was added [16], [51]. The reaction was monitored by TLC, using the solvent system of dichloromethane: methanol / 9.5:0.5 (v/v). The reaction was stopped after 5 days, by filtering the mixture through filter paper and adsorbing the products on Silica (~ 8 g). The purification was carried out by Flash chromatography, on a silica column (Redisep, 24 g), using an isocratic elution of 2 % of methanol in dichloromethane. The combined fractions were analysed by supercritical fluid chromatography (SFC), and the first fraction (633.2 mg) was found pure that was later also confirmed by NMR.

For the easier understanding, we used for methyl *p*-coumarate **pcm** (**1**) and for methyl caffeate **cm** (**5**) abrreviations, as these compounds were used as starting materials in most of our oxidative reactions.

3.3 Oxidation of methyl *p*-coumarate

3.3.1 Oxidation of methyl *p*-coumarate for biological screening

Pcm (**1**) was oxidized under different conditions as a preliminary experiment. An amount of 10.0 mg of **pcm** was dissolved in 10 ml of acetonitrile (OX1), a mixture of acetonitrile and water (9:1, v/v) (OX2), methanol (OX3), a mixture of methanol and water (9:1, v/v) (OX4), or dichloromethane (OX5). A quantity of PIFA (48.3 mg, 2 eq.) (OX1-4) or pyridinium chlorochromate (PCC; 18.1 mg, 1.5 eq.) (OX5) was added to the solutions. The reactions were monitored by thin layer chromatography and stopped after 1-4 hours. After vacuum evaporation, the reactions were adsorbed onto silica (2.0 g), layered above 2.5 g of silica, eluted with 100 ml of ethyl acetate, then evaporated under vacuum. Each reaction mixture was re-dissolved in methanol and submitted to analysis by HPLC1, on a Kinetex XB-C18 (5 μm, 100 Å, 250x4.6 mm) column, using Solvent system 1 at a flow rate of 1 ml/min.

3.3.2 Preparation of oxidized methyl *p*-coumarate derivatives

500 mg (**A**) or 200 mg (**B**) of **pcm** was dissolved in 50 ml of anhydr. acetonitrile (**A**) or in 10 ml of a mixture of acetonitrile and water (9:1, v/v, (**B**)), and 2 eq. of PIFA (2413.3 mg (**A**), 965.3 mg (**B**)) was added. The reaction mixtures were continuously stirred on 60 °C for 5 hours (**A**), or 8 hours (**B**), then evaporated, re-dissolved in methanol, and adsorbed onto 12 g of silica. Flash chromatography was used as the first step of the purification, when dry-loading technique, a silica column (RediSep, 24 g), and a gradient elution of ethyl acetate in *n*-hexane was used from 0 to 100 % at flow rate of 35 ml/min. The collected fractions were combined based on TLC fingerprints. Of the reaction **A**, compound **6** (19.8 mg) was found in pure form after Flash purification. Compound **5** (**cm**) (5.0 mg) was purified with the help of preparative HPLC2, with an isocratic elution of 45% acetonitrile in water, detected on 320 nm. Of the reaction **B**, with the help of preparative HPLC2 compound **7** (6.0 mg) was purified with an isocratic elution of 28% acetonitrile in water, detected on 280 nm, and compound **8** (18.9 mg), with an isocratic elution of 30% acetonitrile in water, detected on 280 nm.

Compound **9** was isolated in low yield (2.43 %) from the reaction of **pcm** (200 mg in 200 ml of acetonitrile) with PIFA (2 eq.). With an aim to increase the yield, other hypervalent iodine compound, PIDA was used as oxidant. 200 mg of **pcm** was dissolved in 200 ml of acetonitrile and water (9:1, v/v), 2 eq. of PIDA (723.0 mg) was added with continuous stirring. After 1-

hour reaction time, the reaction mixture was evaporated under vacuum, and adsorbed onto 3 g of Celite 545. The purification was started with Flash chromatography, using dry-loading technique, a silica column (Redisep Gold, 12 g), and a gradient elution of ethyl-acetate in *n*-hexane from 0 to 100 % at flow rate of 30 ml/min. After the collected fractions were combined based on TLC fingerprints, compound **9** was purified with the help of preparative HPLC2 with an isocratic elution of 42% acetonitrile in water. With this method, 43 mg (yield 19.73%) of compound **9** was obtained.

3.4 Preparation of dearomatized *p*-coumaric acid derivatives

Preparation of *p*-quinols and their *O*-alkyl ethers

The *p*-coumarate esters (**1-4**) were dissolved in acetonitrile: R-OH (9:1, v/v; R-OH: water, butanol or propargyl-alcohol) at a concentration of 1 mg/ml. An amount of 2 eq. of PIDA (*p*-quinols) or PIFA (*O*-alkyl ethers) was added to the solution with continuous stirring on room temperature. The reaction mixture was evaporated after the starting material was not anymore detectable by TLC, then re-dissolved in methanol, and adsorbed onto silica (~ 4 g, Geduran Si 60 Silicagel, 40-63 μm, Merck, Darmstadt, Germany; Silicagel 60, 45-63 μm, Molar Chemicals, Halásztelek, Hungary) or Celite 545 (0.02- 0.1 mm, Merck, Darmstadt, Germany). Flash chromatography was used for the purification on silica column (Redisep Gold 12 g or Redisep 4 g), using a dry-loading technique, with a gradient elution of ethyl-acetate in *n*-hexane from 0 to 100 % at a flow rate of 30 ml/min or 18 ml/min. The fractions were combined based on their TLC fingerprints. Compounds **10**, **11**, **13**, **15**, **17**, **19** and **20** were isolated in pure form with the help of Flash chromatography. The purification of compound **12** was carried out with semi-preparative HPLC3, on a Luna C18 (5 μm, 100Å, 250x10 mm) column, with the isocratic elution of 32 % acetonitrile in water at the flow rate of 2.5 ml/min. Compound **14** was purified with semi-preparative HPLC2 with isocratic elution of 50 % aqueous acetonitrile. Two more compounds were purified with the help of semi-preparative HPLC3 on a Luna C18 (5 μm, 100Å, 250x10 mm) column; compound **16** with isocratic elution of 60 % acetonitrile in water, and compound **18** with 62 % acetonitrile in water, at the flow rate of 2.5 ml/min.

Analytical high-performance liquid chromatography was used for checking the purity of the synthesized compounds by HPLC1 on a Kinetex XB-C18 (5 μm, 100 Å, 250x4.6 mm) column, and by HPLC3 on a Luna C18 (5 μm, 100 Å, 250x4.6 mm) column, using Solvent system 1.

3.5 Preparation of peroxynitrite- and AAPH-oxidized cinnamic acid derivatives

3.5.1 Continuous-flow preparation of peroxynitrite and its reaction with hydroxycinammic acids

The experimental setup of the continuous-flow system, in which peroxynitrite was prepared and reacted with the hydroxycinnamates (**pcm** and **cm**), is presented in Figure 7, in Section 4.4.1. A mixture of 0.6 M H_2O_2 and 0.7 M HCl solution was pumped from Pump1 with a flow rate of 1.5 ml/min. A solution of 0.6 M $NaNO_2$ was pumped from Pump2 with the same flow rate. The two channels were mixed in the first junction, then in the second junction a solution of 1.0 M NaOH was mixed in, that was pumped from Pump3 with a flow rate of 1.5 ml/min. A mixture of the starting material (**pcm** (**1**) or **cm** (**5**)) and 0.1 M glycine buffer was pumped from Pump4, and mixed with peroxynitrite in the third junction. The reaction took place instantaneously. The reaction mixture was collected in a chilled flask placed at the end of a 0.5 ml loop. All tubes of the system were kept in an ice bath (at 0 °C).

3.5.2 Preparation of peroxynitrite-oxidized methyl *p*-coumarate derivatives

The analytical investigation of the reaction mixture was carried out on LC-DAD-MS. A Cortecs (C18, 150x4.6, 2.7 μm) column was applied for the analysis, kept on 40 °C with a mobile phase flow rate of 1.2 ml/min. Gradient elution was used with the following program: solvent B (0.1 % TFA in acetonitrile:water (95:5, v/v)) was gradually increasing in solvent A (0.1 % TFA in H_2O) from 0 % to 40 % in 10 minutes, to 55 % from 10 to 11 minutes, and to 100 % till 20 minutes, washed with 100 % from 20 to 22 minutes, and decreasing back to 0 % at the end.

The purification of the reaction mixture (**pcm** (**1**) reacted with peroxynitrite) was carried out with the help of Sándor Lévai (Gedeon Richter Plc., Budapest, Hungary), on a preparative HPLC4, using a Chromolith C18 (100x4.6, monolithic) column on 40 °C with the flow rate of 30 ml/min. A gradient elution of acetonitrile in water from 0 % to 90 % in 10 minutes was used, then the column was washed with 90 % from 10 to 15 minutes, and with 0 % at the end. With this method compounds **7** and **21** were purified. When the reaction was repeated, small differences were experienced in the product profile, therefore the purification process needed to be modified. A Chromolith and a Reprosil Chiral-Mix (100x4.6 mm, 5 μm) columns were connected one after the other in the HPLC, however the solvent system, column temperature and flow rate was the same. This way compounds **22** and **23** were purified. The reaction mixture was dried under nitrogen stream before the purification, dissolved in 10 ml of acetonitrile, filtered on syringe filter. After it was re-dissolved in 1.5 ml of acetonitrile, 200 or 300 μl was

injected. All the collected fractions were lyophilized overnight to remove solvents. Compounds **7** and **21-23** were obtained and determined, with the following yields from two separate reactions: 0.43 mg (0.35%), 0.59 mg (0.70%), 0.48 mg (3.6%) and 0.40 mg (2.9%), respectively.

3.5.3 Preparation of peroxynitrite and AAPH-oxidized crude product mixtures for bioactivity screening

In the continuous-flow system, amounts of 50 mg of **pcm** (**1**) and **cm** (**5**) were reacted with peroxynitrite. Same aliquots (0.7 ml) of each reaction mixture were dried under nitrogen stream, dissolved in ethyl acetate (2 ml), and extracted three times with water (3x2 ml). The water phase was washed once with ethyl acetate (5 ml), and this organic phase was dried with anhydrous $MgSO_4$, then the solvent was evaporated with nitrogen stream.

Solutions were prepared of **pcm** (**1**) and **cm** (**5**) at 10 mg/ml concentration: 5 mg of the starting material was dissolved in 0.5 ml of the mixture of acetonitrile and water (1:1 or 9:1) or of the mixture of methanol and water (1:1). Compounds were reacted with a solution of 2,2′-azobis(2-methylpropionamidine) dihydrochloride (AAPH), dissolved in the same solvent system at 10 mg/ml concentration. Before the reaction was started, an additional 0.5 ml of water was needed to add to the solutions (acetonitrile:water / 9:1) due to solubility issues with AAPH, therefore the concentrations and solvent compositions were modified accordingly. The reactions were heated on 60 °C in an ultrasonic bath for 4 hours, and after pre-purified as described above.

Samples were analyzed by LC-DAD-MS on a Cortecs (C18, 150x4.6 mm, 2.7 μm) column with a gradient elution of solvent B (0.1 % TFA in a mixture of acetonitrile and water /95:5/) in solvent A (0.1 % TFA in water) from 0 % to 100 % in 10 minutes, then the column was washed with 100 % of solvent B from 10 to 12 minutes.

3.5.4 Longitudinal study of the reaction between methyl caffeate and AAPH

An amount of 50 mg of **cm** (**5**) was dissolved in a 5 ml mixture of acetonitrile and water (9:1, v/v). An amount of 100 mg of AAPH was dissolved in the same solvent as the starting material at 10 mg/ml concentration, and an additional 2.5 ml of water was added to get a clear solution; this was then added to the solution of **cm** (**5**). The reaction was performed by stirring at 60 °C in an oil bath. At specified times, aliquots of 1.4 ml were taken out of the reaction mixture. The first sample was taken out immediately after the reagent was added to the solution (i.e., t_0), subsequent samples were taken at 1, 4, 8, 24, 30 and 48 hours. The reaction was monitored by TLC, using a normal-phase silica gel plate and dichloromethane – methanol

(9.5:0.5, v/v) as solvent system. As visual observation, the initial yellow color of the solution changed to red through orange during the reaction.

Each sample was dried under nitrogen stream, dissolved in 2 ml of ethyl acetate, and washed three times with water (3x2 ml). Water phase was washed once with 5 ml of ethyl acetate, and the combined organic phase was dried with nitrogen. Chromatographic fingerprints of the samples were taken by HPLC1, using a Kinetex Biphenyl (5 µm, 100 Å, 250x4.6 mm) column with a gradient elution of acetonitrile in water from 30 % to 70 %. Samples were also analyzed by SFC.

3.5.5 Isolation of AAPH-oxidized methyl caffeate derivatives

An amount of 100 mg of **cm** (**5**) was dissolved in 10 ml of the mixture of acetonitrile and water (9:1). 200 mg of AAPH was dissolved in 20 ml of the same solvent system, and an additional 5 ml of water was added due to solubility issues. The reaction was stirred and heated on 60 °C in an oil-bath for 24 hours, then cooled down for room temperature, dried under nitrogen stream, dissolved in ethyl acetate (2 ml), and extracted three times with water (3x10 ml). The collected water phase was washed once with 30 ml of ethyl acetate. The organic phase was dried with anhydrous Na_2SO_4, and by nitrogen. Five fractions were purified of the reaction mixture by preparative HPLC5, on a Kinetex biphenyl preparative HPLC column (5 µm, 100 Å, AX, 250 x 21.2 mm), with an isocratic elution of 36 % acetonitrile in water, at the flow rate of 15 ml/min. The purity of the fractions was investigated by HPLC1 system on a Kinetex Biphenyl column (5 µm, 100 Å, 250 x 4.6 mm) at the flow rate of 1 ml/min. Each fraction was tested for their cytotoxic effect, to allow the isolation of cytotoxic compounds. For the fraction (16.0 mg) containing mainly compound **24**, repeated HPLC purification was carried out by HPLC1, using high loading of the Kinetex Biphenyl (5 µm, 100 Å, 250 x 4.6 mm) column with isocratic elution of 34 % of acetonitrile in water at the flow rate of 1 ml/min. With this method, compound **24** (9.3 mg, 18.5%) was obtained at a purity of > 95 %. Compound **25** (2.2 mg, 4.38%) was purified from another HPLC fraction (7.4 mg) by SFC.

3.6 Structure elucidation

Structural characterization of compounds **7**, **8** and **21-25** was performed in collaboration with Dr. Zoltán Béni and Dr. Miklós Dékány (Spectroscopic Research, Gedeon Richter Plc., Budapest, Hungary) by HRMS, NMR and MS/MS spectroscopic methods.

HRMS analyses for compound **8** were performed on an LTQ FT Ultra (Thermo Fisher Scientific, Bremen, Germany) system. HRMS and MS/MS analyses for compounds **7** and **21-25** were carried out on a Thermo Velos Pro Orbitrap Elite (Thermo Fisher Scientific) system.

The samples were dissolved in methanol prior the analysis. The electron spray ionization method (ESI) was operated in positive ion mode (**8**), or either in positive or negative ion mode (**7**, **21**-**25**). The protonated molecular ion peaks were fragmented by collision induced dissociation (CID), and in the case of MS/MS spectra, at a normalized collision energy of 35-45%, using helium as collision gas. Data acquisition and analysis were performed with Xcalibur software version 2.0 (**8**) and version 4.0 (**7**, **21**-**25**) (Thermo Fisher Scientific).

NMR spectra of compound **8** was recorded at 25 °C on a Varian 800 MHz spectrometer equipped with a ^{13}C sensitivity enhanced salt tolerant $^{1}H/^{13}C/^{15}N$ cryogenically cooled probehead. Sample was dissolved in methanol-d_4 (Eurisotop, France). Standard one and two-dimensional spectra were acquired using pulse sequences available in the VNMJ 3.2 library. Chemical shifts are reported in the delta scale using residual solvent signals (methanol-d_4: 3.31 or 49.15 ppm, acetone-d_6: 2.05 or 29.84 for ^{1}H or ^{13}C) as references. ACD/NMR Workbook 2015.2.9 software suite (ACD/Labs, Canada) was used for spectral analysis and data reporting.

NMR spectra for compounds **7** and **21**-**25** were recorded on a Bruker 500 MHz (Billerica, MA, USA) spectrometer equipped with a TCI cryoprobe operating at 499.9 MHz for ^{1}H and 125.7 MHz for ^{13}C, at 25 °C. Chemical shifts were referenced to TMS or residual solvent signals (3.31 (^{1}H)/49.15 ppm (^{13}C) in the case of MeOD-d4,77.0 ppm (^{13}C) in the case of $CDCl_3$, and 1.95 (^{1}H)/1.39 ppm (^{13}C) in the case of acetonitrile-d3). Standard one- and two-dimensional spectra were collected, using the pulse sequences available in the Bruker Topspin 3.5 sequence library. NMR assignments for all isolated compounds were in good agreement with the data reported earlier.

NMR spectra of compounds **5**, **6**, **7** and **9** were recorded on a Bruker Avance NEO 500 MHz spectrometer equipped with a Prodigy BBO 5mm CryoProbe. Compounds **5**, **6** and **9** were dissolved in acetone-d_6, compound **7** was dissolved in methanol-d_4 (VWR Chemicals, Belgium). MestReNova *v*6.0.2-5475 software was used for the evaluation of the recorded standard one and two-dimensional spectra.

NMR spectra for compounds **2**-**4** and **10**-**20** were recorded on a JEOL JNM-ECS 400 MHz (Tokyo, Japan) spectrometer. Samples were dissolved in methanol-d*4*.

3.7 Biological evaluation of the oxidized isolated compounds

3.7.1 Chemicals, cell lines and cell culture conditions

Dulbecco's modified Eagle's medium (MEM), RPMI 1640 medium, fetal bovine serum (FBS), penicillin-streptomycin solution, antibiotic-antimycotic solution, L-glutamine and trypsin/EDTA were purchased from Bioind (Beit Haemek, Israel). Dimethyl sulfoxide (DMSO)

was obtained from Sigma-Aldrich (Munich, Germany), and MTT from Sigma (St. Louis, MO, USA). Annexin-V-FITC (AV) apoptosis detection kit with Propidium Iodide (PI) was purchased from Abcam (Cambridge, UK). Dihydroethidium (DHE) was obtained from Molecular Probes (Invitrogen, USA). Phospho-histone H2A.X antibody and secondary antibody Alexa Fluor 488 goat anti-Rabbit IgG (H + L) were purchased from Cell Signaling Technology Inc. (Danvers, MA, USA).

Two mouse lymphoma cell lines were used: L5178 mouse T-cell lymphoma cell line (ECACC catalog number: 87111908, U.S. FDA, Silver Spring, MD, U.S.), and its multidrug resistant ($L5178_{B1}$) derivative obtained by transfection with pHa MDR1/A retrovirus [52]. Cells were cultured in McCoy's 5A media supplemented with L-glutamine, penicillin, streptomycin, nystatin and inactivated horse serum. Cell culturing was carried out at 37 °C in humidified air containing 5 % CO_2. $L5178_{B1}$ cell line was selected by culturing the infected cells with 60 μg/L colchicine (Sigma).

NCI-H460, NCI-H661, A549 and SiHa cell lines were purchased from the American Type Culture Collection (Rockville, MD, US). HaCaT cell line was obtained from CLS-Cell Lines Service (Eppelheim, Germany). NCI-H460/R cells were derived from NCI-H460 cells after a 3 months-long adaption to doxorubicin. HeLa and MCF-7 cell lines were purchased from Bioresource Collection and Research Center (BCRC, Taiwan). NCI-H460, NCI-H460/R, NCI-H661 and A549 cells were cultured in RPMI 1640 medium supplemented with 10 % inactivated FBS, 2 mM L-glutamine, 10,000 U/ml penicillin, 10 mg/ml streptomycin, 25 μg/ml amphotericin B. HaCaT cells were cultured in DMEM supplemented with 10 % FBS, and the media contained 2 mM L-glutamine, 4.5 g/L glucose, 5000 U/ml penicillin and 5 mg/ml streptomycin. Cell lines were cultured on 37 °C in a humidified 5 % CO_2 atmosphere. Adherent cell lines were sub-cultured at 72 h intervals using 0.25 % trypsin/ EDTA and seeded into a fresh medium as the followings. In case of NCI-H460, NCI-H460/R and HaCaT cell lines, 8000 cells/cm^2, and 16000 cells/cm^2 of H661 were seeded. HeLa, MCF-7 and SiHa cell lines were cultured in Dulbecco's modified Eagle's medium (Sigma-Aldrich) supplemented with 10 % FBS, L-glutamine and 4500 mg/L glucose. These cells were cultured on 37 °C in a humidified incubator containing 5 % CO_2.

The human gynecological cancer cell lines isolated from cervical adenocarcinoma (HeLa) and from breast cancers (MCF7 and MDA-MB-231) were purchased from the European Collection of Cell Cultures (Salisbury, UK), while the cervical carcinoma (SiHa) was obtained from the American Type Tissue Culture Collection (Manassas, Virginia, USA). All media and supplements were ordered from Lonza Group Ltd. (Basel, Switzerland). All the cells were

maintained in Minimum Essential Medium, supplemented with 10% FBS, 1% non-essential amino acids, and 1% penicillin-streptomycin at 37 °C in a humidified atmosphere.

3.7.2 Cytotoxicity testing by MTT assay

MTT [3-(4,5-dimethylthiazol-2-yl)-2,5-diphenyltetrazoliumbromide] assay was used for measuring cell viability, performed in scientific collaboration with Dr. Ana Martins (Institute of Medical Microbiology and Immunobiology, University of Szeged, Szeged, Hungary) on L5178 and $L5178_{B1}$ cells, with Prof. István Zupkó and Dr. Ahmed Dhahir Latif (Department of Pharmacodynamics and Biopharmacy, University of Szeged, Szeged, Hungary) on human adherent gynecological cancer cell lines (HeLa, SiHa, MCF-7, MDA-MB-231), and with Dr. Milica Pešić and Dr. Sonja Stojković Burić (Institute for Biological Research "Siniša Stanković", Belgrade, Serbia) on lung carcinoma cell lines (A549, NCI-H661, NCI-H460, NCI-H460/R). In the case of L5178 and $L5178_{B1}$ cell lines, 6×10^3 cells were added into 96-well flat-bottom microtiter plates, treated with the samples, and incubated for 72 h. Adherent cells grown in 25 cm^2 tissue flasks were trypsinized, seeded into flat-bottomed 96-well tissue culture plates (1000 cells/well for NCI-H460, NCI-H460/R, HaCaT and A549 cell lines, 2000 cells/well for NCI-H661 cell line). The cells were incubated in 100 µl of the appropriate medium overnight, and after 24 h they were treated with compound **8** (1-20 µM) or **9** (1-20 µM), and incubated for 72 h. In the case of gyneological cancer cell lines, 5000 cells/well were seeded in 96-well plates, 100 µl of new media was added after 24 hours, and incubated for 72 hours under cell-culturing conditions, as it was published before [53]. Media contained test samples (longitudinal study, **cm**, **24**) at 0.02-15 µM concentration. MTT was added to each well at the end of the incubation time in a concentration of 0.2 mg/ml or 5 /ml, and incubated for 4 h. Formazan product was extracted from cells by DMSO, and the absorbance was measured by automatic microplate reader (LKB 5060-006 Micro Plate Reader, Vienna, Austria) at 540 or 545 nm. IC_{50} values were defined as the concentration of the drug that inhibited cell growth by 50 % and calculated with the help of GraphPad Prism 5.01 software (GraphPad Software Inc., San Diego, CA, USA) using non-linear regression model log (inhibitor) vs. normalized response and variable slope fit. Two independent *in vitro* experiments were performed with at least five paralell wells. As the concentrations were calculated with the molecular mass of the starting material (**pcm** or **cm**), IC_{50} values were expressed as parent compound equivalents.

3.7.3 Cell death analysis

Cell death analysis was performed in research collaboration with Dr. Milica Pešić and Dr. Sonja Stojkovic Buric. SAV/PI labeling was used to determine the percentages of apoptotic, necrotic and viable cells. Cell lines were incubated overnight in adherent 6-well plates as the folowings: 100 000 cells/well for NCI-H460, NCI-H460/R, HaCaT and A549, 200 000 cells/well for NCI-H661. All cell lines were treated with 10 μM of compound **8** or compound **9**. All the cells (attached and floating) were collected, and the cell pellet was resuspended in 50 μl of binding buffer containing AV and PI in a ratio of 1:1 (v/v). The cells were incubated for 10 minutes at room temperature in dark, and then 1 ml of PBS (phosphate-buffered saline) was added. AV/PI staining was analyzed within 1 h by flow cytometry. CyFlow Space flow cytometer (Partec, Münster, Germany) was used for measuring the fluorescence intensity of AV (FL1-H channel) and PI (FL2-H channel). A minimum of 10,000 events were assayed for each sample. Percentages of apoptotic, early apoptotic (AV+ PI-), viable (AV- PI-), necrotic (AV+ PI+) and dead (AV- PI+) cells were analyzed.

3.7.4 Detection of DNA damage and intracellular ROS levels

Flow cytometry analysis was performed in scientific collaboration with Dr. Milica Pešić and Dr. Sonja Stojković Burić. Cell lines were incubated for 24 hours in adherent 6-well plates as the followings; 100 000 cells/well for NCI-H460, NCI-H460/R, A549 and HaCaT cells, 200 000 cells/well for NCI-H661 cells. All cell lines were subjected to treatments with 10 μM of compound **8** or **9** that lasted for 24 h. Treatment with 2 μM of cisplatin (CDDP) was used as positive control.

For detection of double strand DNA breaks, cells were labeled with phospho-histone H2A.X (Ser139) antibody coupled with secondary antibody Alexa Fluor 488 goat anti-Rabbit IgG (H + L). Adherent cells were harvested by trypsinization, then washed twice in PBS, and fixed in 4 % of paraformaldehyde for 10 min at room temperature. Cells were permeabilized with the addition of ice-cold 90 % of methanol and kept overnight at -20 °C. Cells were washed in PBS, blocked for 60 min with 0.5 % of bovine serum albumin in PBS, and then re-suspended in 100 μl of primary antibody diluted with 0.5 % of bovine serum albumin (1:1000) and incubated for 60 min at room temperature. After washing in PBS, cells were re-suspended in 100 μl of secondary antibody (1:1000) and incubated for 30 min at room temperature.

For detection of ROS levels, cells were stained with superoxide indicator DHE. Adherent cells were harvested by tripsinization and incubated in medium with 1 mM DHE for 30 min at 37 °C in dark. Before measurements, cells were washed and re-suspended in 1 ml of PBS.

Fluorescence intensity of phospho-histone H2A.X (Ser139) antibody coupled with secondary antibody (FL1-H channel) and DHE (FL2-H channel) was measured on CyFlow Space flow cytometer (Partec, Münster, Germany). A minimum of 10 000 events were assayed for each sample.

3.7.5 DNA damage response study

DNA damage response studies were performed in research collaboration with Prof. Hui-Chun Wang and Dr. Ching-Ying Kuo (Graduate Institute of Natural Products, Kaohsiung Medical University, Kaohsiung, Taiwan R.O.C.). MCF-7 cells (700 000 cells/dish) were incubated overnight in adherent 60 mm culture dish, and pre-treated with 10 μM of **pcm** (**1**) or compound **9** for 30 min. Treatment with 10 μM of protoapigenone was used as positive control. Cells were exposed to UV irradiation (10 J/m^2) for 1 hour to induce DNA damage responses (DDR). Protein collection and western blot assays were performed in accordance with the method described formerly [54]. Proteins of the cells were extracted with lysis buffer (1mM EDTA, 10 mM Tris, pH 7.5, 0.5 % NP-40, 10 % glycerol, and 420 mM NaCl) and supplemented with a cocktail of protease and phosphatase inhibitor (Roche Applied Science), and 1 mM DL-dithiothreitol. After SDS-PAGE, the separated proteins in the gel were electrophoretically transferred to nitrocellulose membranes, that were detected with specific primary antibodies followed by horseradish peroxidase (HRP)-coupled secondary antibodies (Jackson ImmunoResearch, Ely, Cambridgeshire, UK), and recognized by Enhanced chemiluminescence (ECL) reagent (Millipore, Sigma-Aldrich). Images were recorded with a LAS-4000 luminescent image analyser system (Fujifilm, Tokyo, Japan). The primary antibodies against Chk1-S345 and Chk2-T68 were purchased from Cell Signaling Technology (Danvers, MA, USA), Chk1, Chk2 and β-actin (that served as an internal control) were ordered from Santa Cruz.

3.8 Investigation of the formation of hydroxycinnamic acid metabolites in biorelevant environment

3.8.1 Combination assay on the cytotoxicity of methyl *p*-coumarate and H_2O_2

To study the interaction between **pcm** (**1**) and H_2O_2 concerning their cytotoxic activity on MCF-7 cells, a checkerboard microplate method was applied in collaboration with Prof. Hui-Chun Wang and Dr. Ching-Ying Kuo. 1×10^4 cells were seeded to each well in a 96-well plate, then the plates were incubated at 37 °C for 24 hours. **Pcm** and the standard solution of H_2O_2 (Sigma-Aldrich) were stored at -20 °C until use. The stock solutions and the serial two-fold dilutions of each drug were prepared according to the recommendations of several fix methyl

p-coumarate and H_2O_2 ratios to testing. **Pcm** was serially diluted along the ordinate, while H_2O_2 along the abscissa. Aliquots of 100 µl (including **pcm** and H_2O_2) were added to each well, then the plates were incubated 37 °C for 4 hours. After the MTT-containing medium was removed, 100 µl of DMSO was added to dissolve the formazan crystals. Determination of cell viabilty was carried out with an ELISA reader (Thermo Multiskan Ascent) by measuring the optical density values (absorbance) of the chromogenic product at 550 nm. Three replicates (prepared on three different days) were utilized to calculate the combination index (CI) values at several fix **pcm** vs. H_2O_2 ratios by using CalcuSyn software.

Stability test of methyl *p*-coumarate in the presence of H_2O_2

An amount of **pcm** (**1**) (1.00 mg) was dissolved in methanol (1 ml) and 400 µl of 30 % hydrogen peroxide was added to the solution with continuous stirring. The reaction was carried out at room temperature in dark. Aliquots of 200 µl were obtained from the mixture at specified times (1 h, 2 h, 24 h, 48 h, 72 h, 92 h), when the reaction was stopped by addition of 4 µl of NaOH (10 %) to get pH 7. Each sample was purified by SPE on silica, washed with ethyl acetate, evaporated under nitrogen stream, re-dissolved in HPLC grade methanol, and analysed by HPLC1 on a Kinetex XB-C18 (5 µm, 100 Å, 250x4.6 mm) column. **Pcm** was stable for as long as 92 hours in presence of H_2O_2.

3.8.2 Cytotoxicity testing of methyl caffeate with or without the presence of *t*-BHP-induced oxidative stress

Cytotoxicity of **cm** (**5**) with or without the presence of *t*-BHP-induced oxidative stress was tested in collaboration with Prof. István Zupkó and Dr. Ahmed Dhahir Latif. Each cell line was tested in six groups, three cell controls and three for treatment. All of them were plated according to the above method described at MTT assay, and treated for 24 hours with medium, or medium containing *t*-BHP at its 1/3 IC_{50} concentration, or medium containing *t*-BHP at its $IC_{50}^{(72h)}$ concentration. After the medium was removed, the cells were washed with PBS, and a new medium was added, with or without **cm** treatment. After 72 hours of incubation, the cells were tested for viability by MTT assay as described above. The IC_{50} value of *tert*-butyl hydroperoxide (*t*-BHP), an oxidative stress-inducing substance was assessed in the same way. The results were statistically analysed by two-way analysis of variance (ANOVA), followed by a Bonferroni post-hoc test, and differences were considered significant at $p < 0.05$.

3.8.3 Fenton reaction of methyl *p*-coumarate

Implementation of the reaction was the same as in the previous Section 3.8.1 (stability test with H_2O_2), but with the difference of the addition of iron(II) sulfate heptahydrate (5 mg).

An aliquot of 200 µl was taken out of the mixture after 30 minutes, and the sample was processed with the same method that is described in Section 3.8.1, and also analysed by HPLC1 on a Kinetex XB-C18 (5 µm, 100 Å, 250x4.6 mm) column. For the HPLC-PDA fingerprint of Fenton reaction of pcm see Section 4.7.3, Figure 16. The reaction was repeated with the same reaction conditions and subjected to HPLC-MS analysis as well. LC-DAD-MS measurement was carried out on a Kinetex EVO C18 (2.6 µM, 50x3.0 mm, Phenomenex) column on 45 °C with a gradient elution of 2-100 % B at 0-5.9 min, 100 % of B at 5.9-7.0, from 7.01 back to 2 % of B at flow rate of 1.25 ml/min. Eluent A: 0.1 % (v/v) trifluoroacetic acid (TFA) in water, eluent B: 0.1 % TFA in the mixture of acetonitrile and water (95:5).

3.8.4 Hydroxyl radical scavenging activity of methyl *p*-coumarate

The ˙OH scavenging capacity was performed in collaboration with Dr. György Tibor Balogh (Compound Profiling Laboratory, Gedeon Richter Plc., Budapest, Hungary, current affiliation: Department of Pharmacodynamics and Biopharmacy, University of Szeged, Szeged, Hungary; and Department of Chemical and Environmental Process Engineering, Budapest University of Technology and Economics, Budapest, Hungary) by measuring the inhibition of damage to 2-deoxy-D-ribose by Fenton reaction [55]. Trolox was used as a positive control. Assays were carried out in 50 mM MOPS buffer, at the pH 6.0, containing 2.8 µM 2-deoxy-D-ribose and increasing concentrations (0.002-5 mM) of samples. 0.2 µM H_2O_2 and 1.5 µM $FeSO_4$ were added to start the reaction (in total volume of 280 µl). After 3 minutes incubation at 37 °C, during which period of time ˙OH formation was linear, TBA (thiobarbituric acid) reactivity was developed by heating at 100 °C for 15 minutes after adding 400 µl of a mixture containing 15 % (w/v) TCA (trichloroacetic acid), 0.325 % (w/v) TBA, 0.25 M HCl and 0.06 M NaOH. Chromogens were detected at wavelength of 532 nm against appropriate blanks [56].

3.8.5 *In silico* studies on the formation of methyl *p*-coumarate metabolites in the presence of ˙OH radicals

In silico calculations were performed in collaboration with Prof. Patrick Trouillas (INSERM UMR 1248 IPPRITT, University of Limoges, Faculty of Pharmacy, Limoges, France; and RCPTM, Faculty of Sciences, Palacký University, Olomouc, Czech Republic) and Dr. Florent Di Meo (INSERM UMR 1248 IPPRITT, University of Limoges, Faculty of Pharmacy, Limoges, France) with the Gaussian09 package (Rev. A). B3P86 functional was chosen for optimization of ground states geometrics as it has been shown to properly reproduce thermodynamics of polyphenol oxidative processes. For describing C-, O- and H-atoms, the double-ζ basis set 6-31+G(d,p) was used in the experiment. Solvation polarization effects were

included in the calculations by using conductor-like polarizable continuum model (C-PCM). To ensure that the obtained geometries were in the global minimum of the potential energy surface, frequency calculations were performed, as pictured by the absence of any imaginary frequency. With the help of VMD program, Mulliken spin density visualization has been carried out.

4. RESULTS

4.1 Preparation of hydroxycinnamic acid esters as starting materials

To avoid decomposition and potential chromatographic challenges connected to the acid function, we decided to use ester derivatives of HCAs to study their oxidations. With the above described procedures (see Section 3.2.2), methyl-, ethyl-, butyl- and isopropyl esters of *p*-coumaric acid (**1-4**), and methyl ester of caffeic acid (**5**) were prepared. Structures of the prepared ester derivatives are shown in Figure 2.

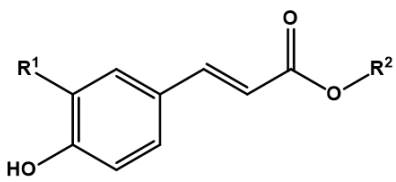

	R^1	R^2
pcm (**1**):	-	Me
2:	-	Et
3:	-	But
4:	-	*i*Pr
cm (**5**):	OH	Me

Figure 2. Chemical structures of the prepared hydroxycinnamic acid esters that were used as starting materials for oxidative transformations.

4.2 PIFA- or PCC-mediated oxidation of methyl *p*-coumarate

We aimed to study the effect of various oxidative conditions on the cytotoxic activity of **pcm** (**1**), therefore, first a series of reaction mixtures were prepared for cytotoxicity screening. The oxidations were carried out with a hypervalent iodine (III) reagent, PIFA, in acetonitrile, in a mixture of acetonitrile and water (9:1, v/v), in methanol, in a mixture of methanol and water (9:1, v/v), or with pyridinium chlorochromate (PCC) in dichloromethane. Each reaction mixture was subjected to solid-phase extraction to purify from residual traces of reagents. The obtained product mixtures (named OX1-5) were submitted to cytotoxic activity testing on a mouse lymphoma cell line pair (L5178 and $L5178_{B1}$).

Of the reaction mixtures, OX1 and OX2 demonstrated a highly increased cytotoxic effect as compared to that of **pcm**, therefore these reaction conditions were selected to perform scale-up reactions to obtain individual active constituents. The oxidation of **pcm** with PIFA was performed in acetonitrile (**A**) or in a mixture of ancetonitrile and water (9:1, v/v) (**B**) with a larger amount of the starting material. After the reaction mixtures were separated to major

fractions by Flash chromatography, compounds **5-9** were purified with the help of preparative HPLC. Characteristic chromatograms of the scaled-up reactions, and the purification proccess are presented in Figure 3.

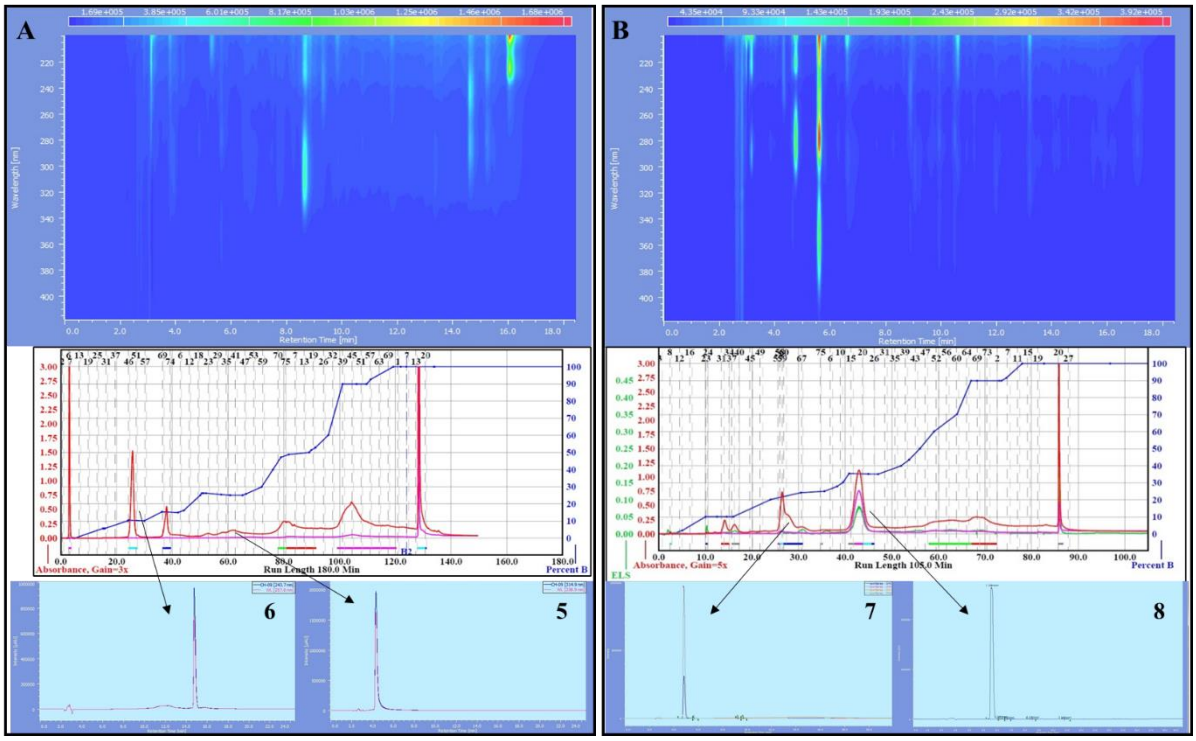

Figure 3. Purification of compounds from the scaled-up oxidative reaction of **pcm** (**1**) with PIFA in acetonitrile (**A**) and in a mixture of acetonitrile and water (9:1, v/v) (**B**). Top pane: HPLC-PDA chromatograms of the crude reaction mixtures; middle pane: chromatograms of the flash purifications, bottom pane: HPLC chromatograms of the purified compounds **5-8**.

Comparing the HPLC-PDA chromatograms of the preliminary oxidations and the scaled-up reactions, we found that the product profile highly depends on the concentration. Therefore, the reaction was repeated with higher amount of **pcm**, but using an other hypervalent iodine reagent, PIDA, and keeping the 1 mg/ml concentration. After the reaction mixture was purified with the help of flash chromatography and preparative HPLC, compound **9** was obtained. HPLC-PDA chromatograms of the reaction and the purified compound **9** are presented in Figure 4.

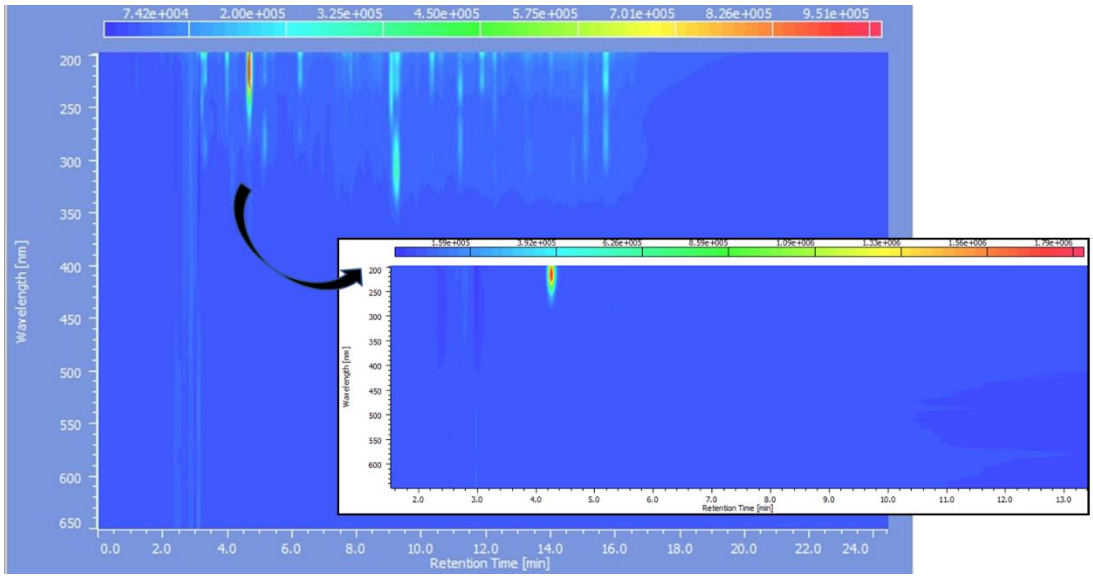

Figure 4. HPLC-PDA chromatogram of the product mixture of **pcm** oxidized with PIFA, that was performed with 1 mg/ml concentration of **pcm**, and of the purified compound **9**.

Compound **9** was isolated in low yield (2.43 %) when pcm was oxidized with PIFA, however when PIDA, another hypervalent iodine reagent was used as oxidant, a better yield (19.73 %) was achieved.

Of all the scaled-up procedures that were performed, altogether 5 oxidized metabolites (**5-9**) were isolated by combined chromatographic techniques. Figure 5 represents the structures of the compounds obtained. For a detailed description of the scaled-up reactions and isolation of the compounds, see Section 3.3.2.

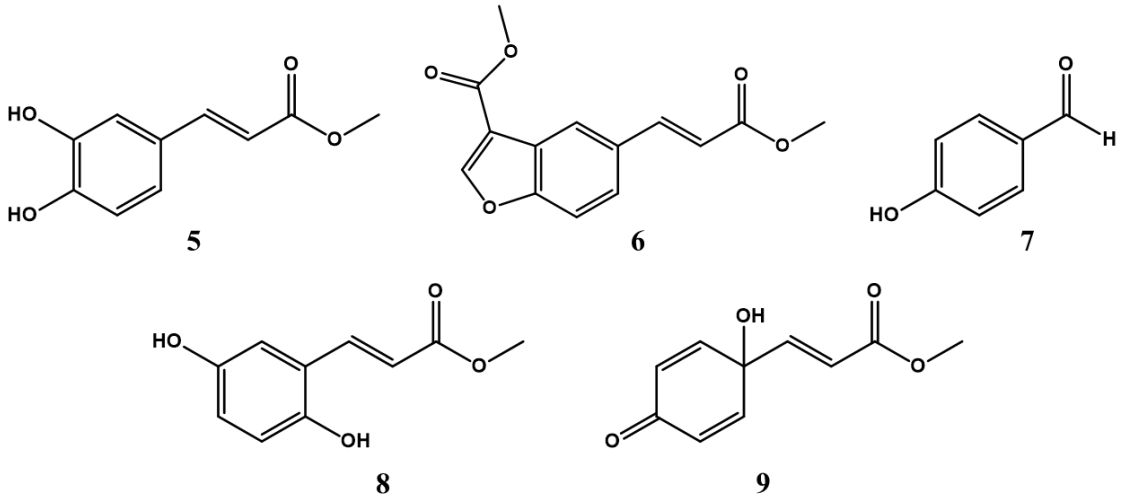

Figure 5. Structures of compounds **5-9** isolated from the oxidation of **pcm** with PIFA.

4.3 Preparation of dearomatized *p*-coumaric acid derivatives with hypervalent iodine reagents: *p*-quinols and their *O*-alkyl ethers

p-Coumarate esters (**1-4**) were oxidized in a mixture of acetonitrile and water (9:1, v/v) with the hypervalent iodine compound PIDA to obtain *p*-quinol derivatives (**9-12**), or in a mixture of acetonitrile and alcohol (butanol or propargyl-alcohol, 9:1, v/v) with the hypervalent iodine compound PIFA, to obtain the corresponding *O*-alkyl ethers (**13-20**). Compounds **10-20** were obtained as new compounds. For the reaction conditions and isolation, see Section 3.4. Figure 6 shows the structures of the starting components (esters) and the prepared oxidized derivatives.

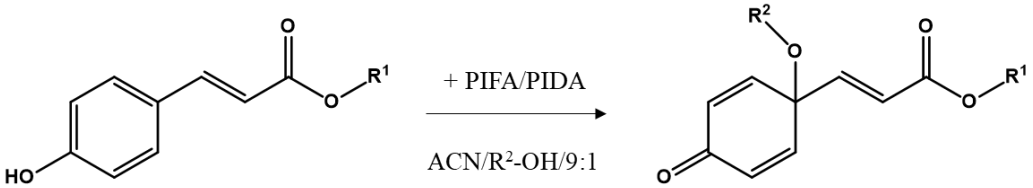

	R^1	R^2		R^1	R^2		R^1	R^2
9:	Me	H	**13**:	Me	But	**17:**	But	But
10:	Et	H	**14**:	Me	Propargyl	**18:**	But	Propargyl
11:	But	H	**15**:	Et	But	**19:**	*i*Pr	But
12:	*i*Pr	H	**16**:	Et	Propargyl	**20:**	*i*Pr	Propargyl

Figure 6. Oxidative dearomatization of *p*-coumaric acid esters (methyl, ethyl, butyl, isopropyl) with hypervalent idodine reagents (PIFA, PIDA). Mixtures of acetonitrile and water or the alcohol corresponding to the R^2 alkyl group (*n*-butanol, propargyl-alcohol) were used as solvents.

4.4 Preparation of peroxynitrite- and AAPH-oxidized cinnamic acid derivatives

4.4.1 In situ continuous-flow oxidative reaction of methyl cinnamates with peroxynitrite

First, a continuous flow reaction (CFR) system was set up to obtain well-controlled reaction conditions for the oxidative reaction between peroxynitrite ($ONOO^-$) and hydroxycinnamic acids (**pcm** (**1**) and **cm** (**5**)). Schematic representation of the continuous flow system is showed in Figure 7.

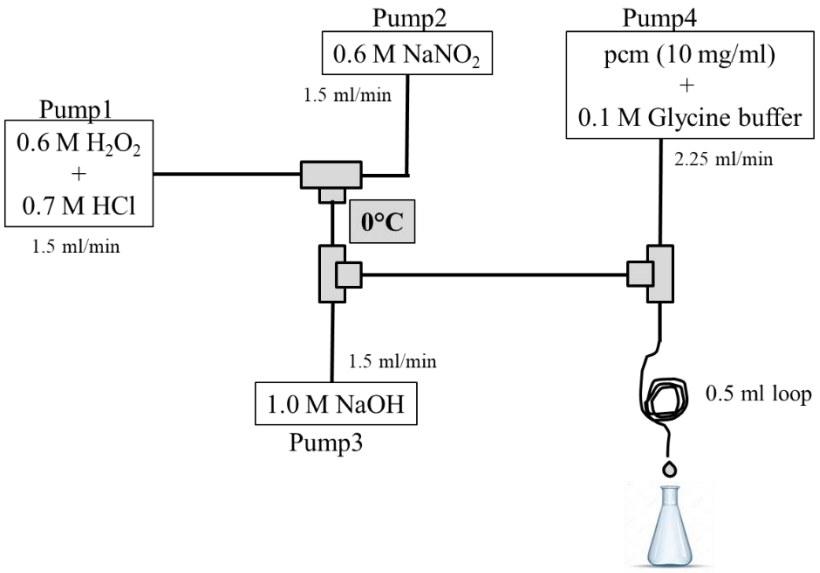

Figure 7. Experimental setup of the continuous-flow system, in which the reaction took place between hydroxycinnamates and the in situ formed peroxynitrite.

At first, **pcm** (**1**) was reacted with $ONOO^-$ in the CF system to test its preparative potential. Altogether four products (**7**, **21-23**) were purified with the help of preparative HPLC, which structures were elucidated by high-resolution mass spectroscopy (HRMS) and comprehensive 1- and 2D nuclear magnetic resonance (NMR) spectroscopic methods. Structures of compounds **7** and **21-23** are presented in Figure 8. Compound **22** was obtained as a new compound.

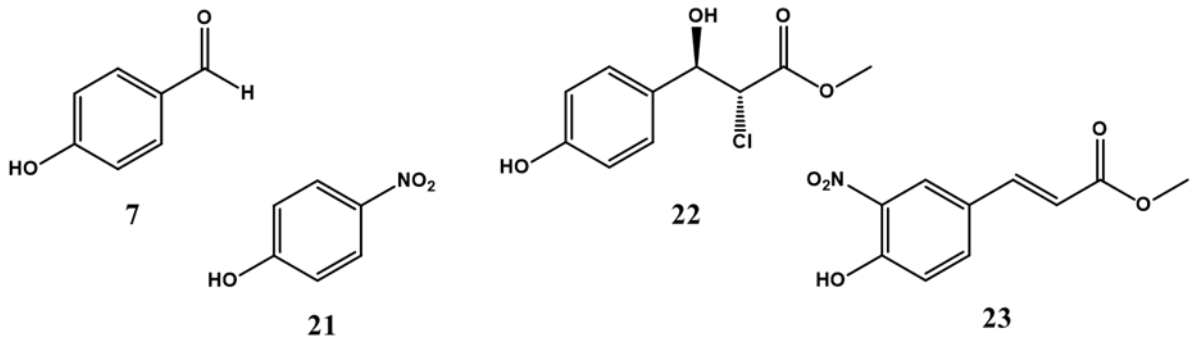

Figure 8. Structures of compounds **7** and **21-23** obtained from the reaction between pcm and peroxynitrite. Only one enantiomer is shown for the racemic compound **22** for clarity.

4.4.2 Preparation of peroxynitrite- or AAPH-oxidized crude product mixtures for bioactivity screening

Our aim was to find ROS/RNS scavenging-related, possibly antitumor metabolites of **pcm** (**1**) or **cm** (**5**), which are formed upon oxidation by $ONOO^-$ or AAPH. All the prepared crude product mixtures were tested for their cytotoxic acitivity on human gynecological cancer cell lines (HeLa, SiHa, MCF7, MDA-MB-231). None of the reaction mixtures of **pcm** showed

potent cytotoxic effect in this investigation, but a significantly increased cytotoxic effect (especially on HeLa cells) was experienced when **cm** was reacted with AAPH.

4.4.3 Longitudinal study of the oxidation between methyl caffeate and AAPH

As the reaction of **cm** (**5**) with AAPH was selected for furter experiments after the bioactivity screening, a longitudinal study was performed to find the best reaction time for the isolation of the cytotoxic constituent(s). Samples were taken out at specified reaction times (i.e. 0, 1, 4, 8, 24, 30 and 48 hours) and analyzed for their product profiles by HPLC and SFC. The samples were tested for their cytotoxic activity on HeLa cells in parallel with the analytical measurements. As the reaction proceeded and the amount of the starting material (**cm**) decreased, the amounts of the products were increased that was accompanied by a gradually increasing cytotoxic activity until 24 hours, then the bioactivity was gradually decreasing. Most important results of this study are summarized in Figure 9.

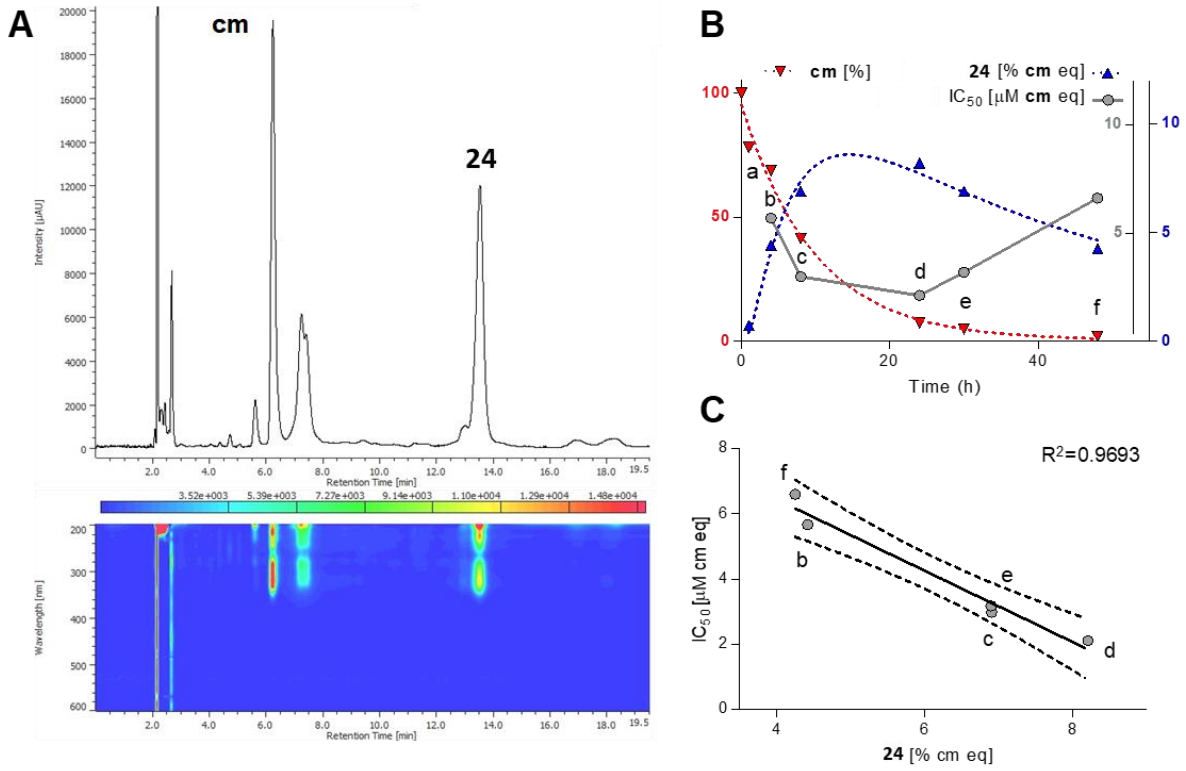

Figure 9. Results of the longitudinal study on the reaction between **cm** and AAPH. (**A**) SFC-PDA fingerprint of the most potent cytotoxic sample taken at 24 h of reaction time; chromatogram represents maximum absorbance in the wavelength range of λ = 350-600 nm. (**B**) Time dependency of the reaction and the IC_{50} values of the respective samples taken at 0 h (t_0), 1 h (a), 4 h (b), 8 h (c), 24 h (d), 30 h (e) and 48 h (f) on HeLa cells. Amounts of compound **24** (right y-axis, blue) and IC_{50} values (right y-axis, grey) of the samples are expressed in cm equivalents (μM and %, respectively), nonlinear regression for the amounts of **cm** (left y-axis, red) and compound **24** was performed by the one-phase decay and the log Gaussian models of GraphPad Prism 5.0, respectively. (**C**) Linear correlation between the relative area under the curve (AUC) values of compound **24** and the IC_{50} values. The 95% confidence interval of the regression line is shown with dashed lines; AUC is given in % relative to that of **cm** at t_0.

4.4.4 Bioactivity-guided isolation of the cytotoxic metabolite(s) of methyl caffeate

Due to the results of the reaction monitoring, the 24-hour reaction time was selected for a scale-up to isolate the effective compound(s). Regardless of the strong positive correlation between the amount of compound **24** and the cytotoxic effect, bioactivity-guided purification strategy was chosen to allow the isolation of further active compounds. First, the reaction mixture was separated to main fractions with the help of preparative HPLC, then each fraction was tested for its cytotoxic activity on HeLa cells. Fraction 3 showed ~80 % inhibiton at 1.8 μM concentration as expressed in methyl caffeate equivalents. Compound **24** was purified of this fraction by HPLC. All other fractions proved to be essentially inactive in the cell viability assay, but fraction 5 was also selected for isolation because of a well-resolved peak of a major compound in it. Compound **25** was purified from this fraction by SFC. Structures of compound **24** and **25** are shown in Figure 10.

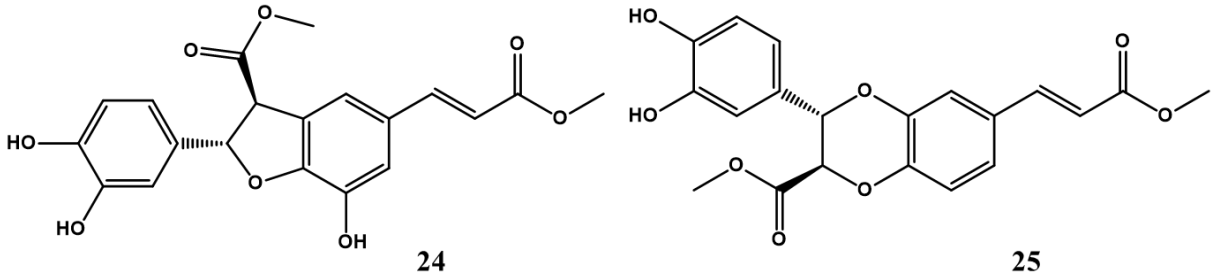

Figure 10. Structures of oxidized products (**24**, **25**) isolated from the reaction of **cm** with AAPH. Both compounds were obtained as racemates; only one enantiomer is shown for clarity.

Compound **24** was also detectable in the product mixture of the reaction between **cm** (**5**) and peroxynitrite, that is demonstrated in Figure 11.

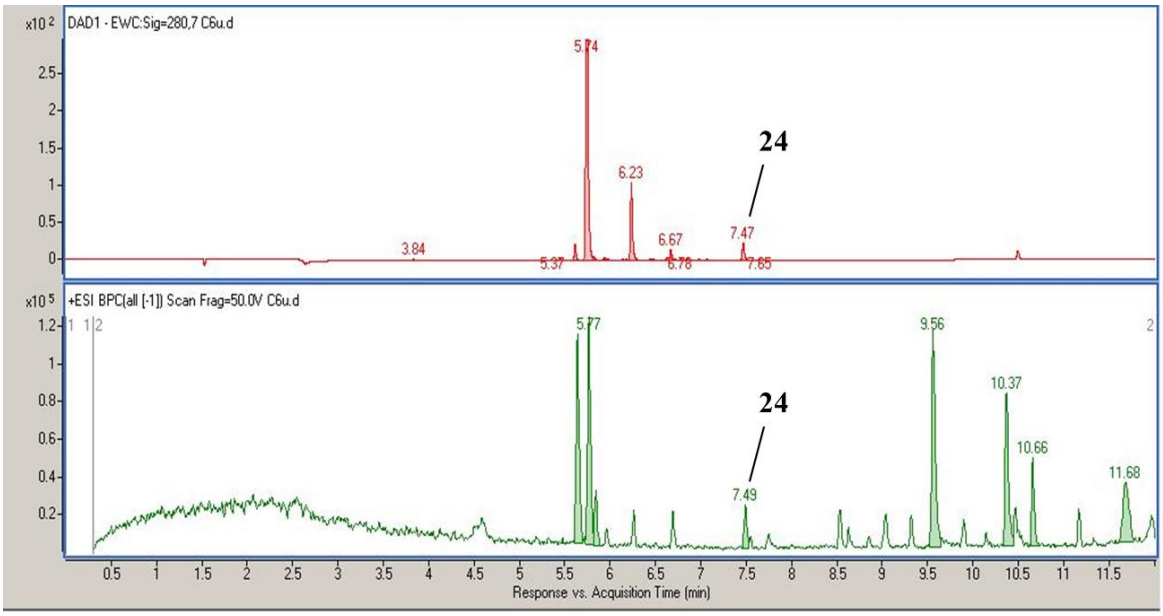

Figure 11. Chromatographic fingerprint of the continuous-flow reaction of **cm** with peroxynitrite. Top pane: PDA detection, λ= 280±7nm; Bottom pane: base peak chromatogram registered from MS/MS detection. Analysis was performed on a Cortecs (C18, 150 × 4.6 mm, 2.7 μm) column with a gradient elution of Solvent B (0.1 % TFA in acetonitrile:water / 95:5) in Solvent A (0.1 % TFA in H_2O) from 0 to 100 % in 10 minutes, and washed with 100 % B from 10 to 12 minutes.

4.5 Stucture elucidation of the oxidized products

In the identification of the *p*-coumaric acid esters (**1-4**), the appearance of the desired alkyl group's characteristic NMR signal patterns in the ^{1}H spectrum confirmed successful esterification.

To identify the corresponding *p*-quinol derivatives (**9-12**), we compared the proton spectras of them with that of the starting material esters. It is presented here through the example of the derivatives of ethyl ester (**10**, **15**) (Figure 12). As the *p*-quinol ring formed, the coupling constant of the 2-2 protons in the cis double bond has changed to *J*= 10.0 Hz, and the other strcutural parts are retained. In the case of buthyl ether derivatives (**13**, **15**, **17**, **19**); protons of the side chain, and a second methyl group appeared around 0.88 ppm. And what indicates the presence of the propargyl side chain in propargyl ethers (**14**, **16**, **18**, **20**) is the one proton around 2.86 ppm.

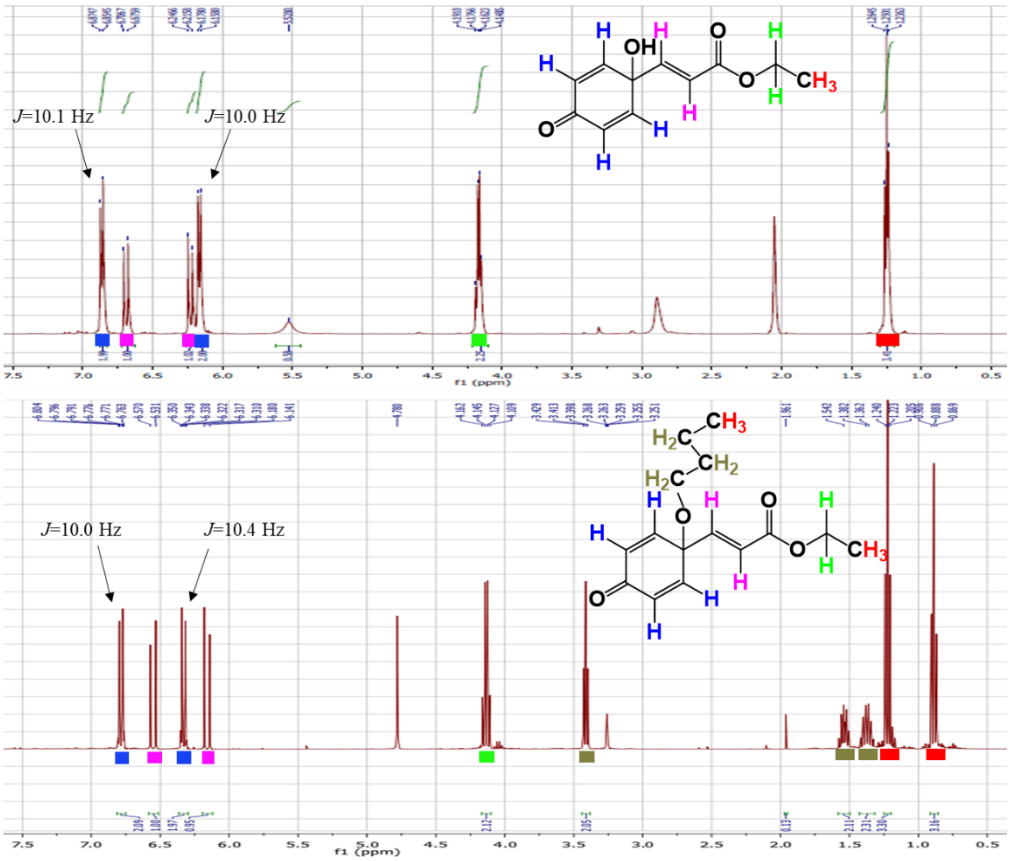

Figure 12. ^{1}H NMR spectra of the *p*-quinol analog (**10**, upper) and buthyl ether derivative (**15**, bottom) of *p*-coumaric ethyl ester. The corresponding protons are marked in the structure and in the spectra.

In the case of compounds **7**, **21** and **23**, the NMR chemical shifts we obtained were in good agreement with those published in the literature [57]–[59]. While compound **22** was obtained as a new compound, stereoisomers of the structurally similar 4-OMe derivative have already been reported in many papers [60]–[62]. Our NMR data were in good agreement with the data published by Matsuki et al. [60]. The observed J = 8.9 Hz coupling constant between H7 and H8, together with the consequences reported by Cabon et al. [63], suggest that compound **22** is the racemic mixture of the anti-isomers represented in Figure 8. The NMR chemical shifts of compounds **24** and **25** showed good agreement with the previously published NMR data for both compounds [16], [64], revealing that they are dimerization products.

4.6 Results of the biological assays

4.6.1 Investigation of the cytotoxic activity of the oxidized methyl *p*-coumarate metabolites by MTT assay

A series of oxidized reaction mixtures of methyl *p*-coumarate were prepared with the aim of studying the effect of various oxidative conditions on its cytotoxic activity (for details see Section 3.3.1). After work-up, each product mixture (OX1-5) was tested for cytotoxic activity

on a mouse lymphoma cell line (L5178) and its mult-drug resistant (MDR) counterpart ($L5178_{B1}$) in comparison with **pcm**. The MDR sub-cell line was previously obtained from L5178 by transfection with the human *ABCB1* gene.

Two product mixtures, OX1 and OX2 showed dramatic increase in the cytotoxic activity as compared to that of **pcm**. Therefore these two reactions were scaled-up in order to obtain the constituents responsible for the effect. Of the performed three scale-up oxidations, altogether 5 metabolites (**5-9**) were isolated which *in vitro* cytotoxic activity was tested on the above described mouse lymphoma cell line pair (L5178 and $L5178_{B1}$). Compounds **8** and **9** were even tested on a various panel of cancer cell lines for their cytotoxic activity, e.g., HeLa, SiHa, MCF-7, and several lung carcinoma cell lines; a highly metastatic large cell lung carcinoma (NCI-H661), A549 adenocarcinoma, and a non-small cell lung carcinoma (NCI-H460) and its multi-drug resistant pair (NCI-H460/R) developed by continuous exposure of the initially sensitive cell line to doxorubicin. Results of the cytotoxic bioassays are summarized in **Figure 13.** This work was performed in collaboration with the group of Dr. Milica Pešić (Institute for Biological Research "Siniša Stanković", Belgrade, Serbia).

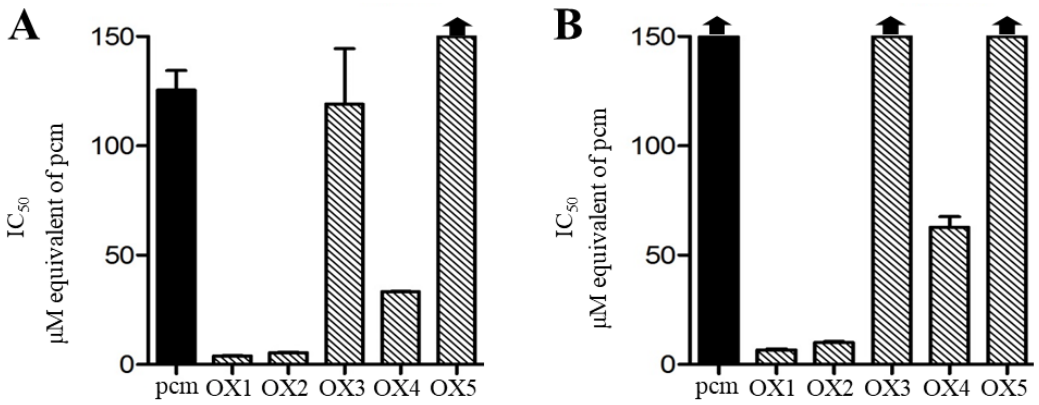

C

	IC_{50} ± SEM (µM)									
	L5178	$L5178_{B1}$	NCI-H460	NCI-H460/R	A549	NCI-H661	HaCaT	MCF-7	HeLa	SiHa
pcm	125.60 ± 8.89	> 150	120.01 ± 2.14	1043.13 ± 59.36	322.92 ± 8.09	289.21 ± 8.42	311.22 ± 3.75	> 400	> 150	> 150
8	5.23 ± 0.29	12.38 ± 0.23	3.77 ± 0.07	7.05 ± 0.13	4.14 ± 0.09	4.19 ± 0.11	9.69 ± 0.18	-	8.51 ± 1.54	-
9	0.46 ± 0.09	0.62 ± 0.08	1.85 ± 0.03	2.06 ± 0.03	4.32 ± 0.09	1.44 ± 0.02	4.05 ± 0.10	6.22 ± 1.07	9.85 ± 1.03	8.89 ± 1.09
Dox	0.41 ± 0.07	11.83 ± 0.64	0.04 ± 0.01	1.89 ± 0.25	0.55 ± 0.16	0.35 ± 0.12	0.03 ± 0.01	1.08 ± 0.01	1.21 ± 0.05	0.76 ± 0.01

Figure 13. Cytotoxic activity of **pcm** and its oxidized metabolite mixtures (OX1-5) on a mouse lymphoma cell line pair: L5178 (**A**) and $L5178_{B1}$ (**B**). Dilutions for each mixture were performed by calculating with the molecular mass of **pcm**; upward arrows mark samples with IC_{50} values > 150 µM. *In vitro* cytotoxic activity of **pcm** and its oxidized metabolites (**8**, **9**) isolated from the scaled-up OX1 and OX2 (**C**). IC_{50} values are given in µM as mean ± SEM from three parallel experiments; Dox: doxorubicin. Compounds **5-7** are not included in this table; due to their >100 µM IC_{50} values on the mouse lymphoma cell lines they were excluded from being tested on further cell lines.

Of all the tested compounds, the parent antioxidant **pcm** exerted the lowest cytotoxic activity. The NCI-H460/R cell line showed nearly 10-fold cross resistance to this compound, comparing to the NCI-H460. The resistance profile of compound **8** was much more favourable on this cell line pair, with a less than twice cross-resistance in the MDR one, while a 2.4 times cross-resistance was observed in the MDR cell line $L5178_{B1}$. Compound **9** was able to bypass resistance of both MDR cancer cell lines ($L5178_{B1}$, NCI-H460/R), and, considering its cytotoxicity on HaCaT keratinocytes, it showed a favorable selectivity profile towards cancer cells.

4.6.2 Cell death analysis of oxidized methyl *p*-coumarate metabolites

After human lung carcinoma cell lines (NCI-H460, NCI-H460/R, A549, NCI-H661) and normal human keratinocytes (HaCaT) were treated with compound **8** and **9**, Annexin-V/PI

staining was used to determine the percentages of apoptotic, necrotic and viable cells. The procedure revealed that both compounds **8** and **9** induce cellular necrosis. After treatment with compound **9**, the percentage of late apoptotic NCI-H661 cells was increased from 0.95 % (untreated control) to 9.57 % (treated), and the percentage of necrotic NCI-H661 cells from 2.58 % (untreated control) to 44.82 % (treated). In HaCat cells treated with the same dose of compound **9**, the percentage of viable cells was 91.50 %, also suggesting the selectivity of compound **9** towards cancer cells.

4.6.3 DNA damage studies

Investigation of DNA damaging effect and the effect on DNA damage response

After treatment with compound **8** or **9**, the expression of Histone 2A.X (H2A.X) was analysed as a marker of DNA damage. The potential effect of compound **9** on DNA damage response was evaluated with Western immunoblotting after UV irradiation of MCF-7 cells. Results of the DNA damage studies are presented in Figure 14.

Compound **9** induced DNA damage in NCI-H460 and NCI-H460/R cells with a significantly increased expression of H2A.X, but it was decreased in normal HaCaT cells after treated with compound **9**. Compound **8** reduced the expression of H2A.X in most of the cancer cells and even in HaCaT cells (Figure 14A). The evaluation of ROS production was carried out by dihydroethidium labelling. Compound **9** caused a significant increase of ROS levels in A549, NCI-H460 and NCI-H661 cells, however a decrease was observed in NCI-H460/R and HaCaT cells. Compound **8** decreased the level of ROS in all tested cancer cell lines and also in HaCaT keratinocytes (Figure 14B). The positive control, cisplatin (CDDP) significantly increased the ROS levels in HaCaT cells, but not in NCI-H460 cancer cells, suggesting a better selectivity profile of compound **9**. This work was performed in collaboration with the group of Dr. Milica Pešić (Institute for Biological Research "Siniša Stanković", Belgrade, Serbia).

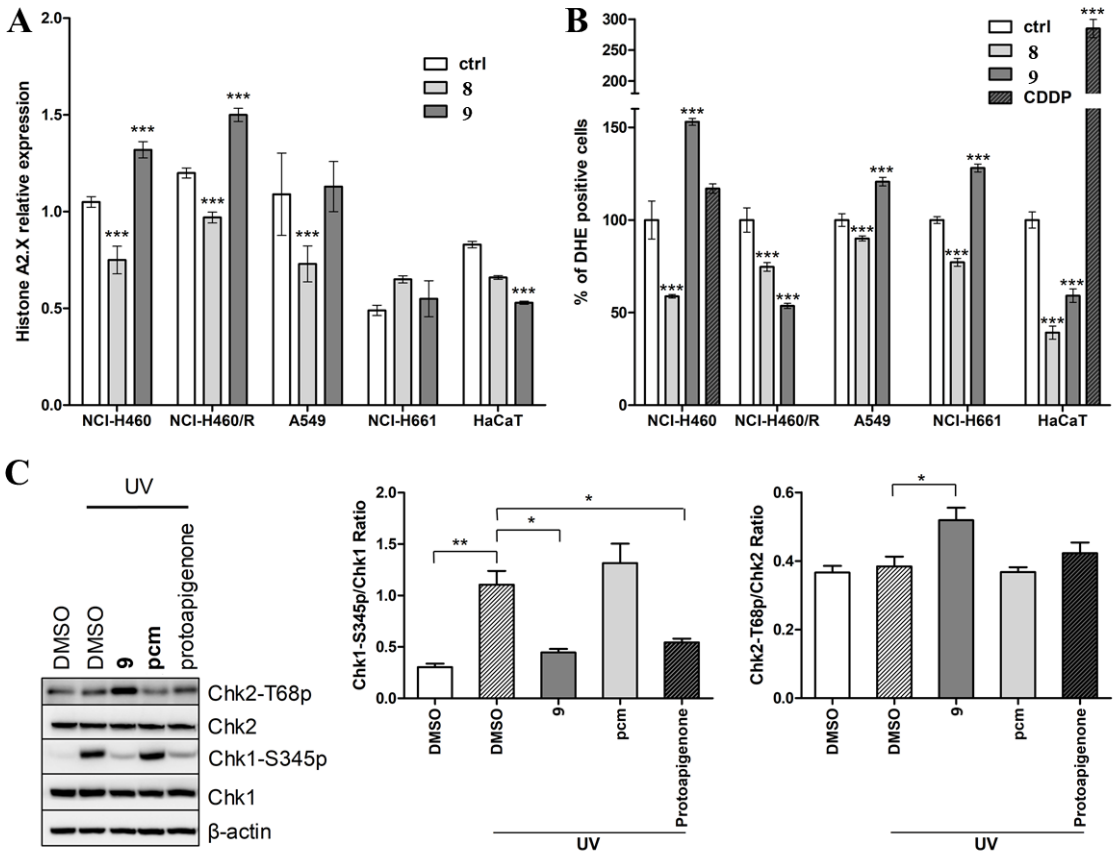

Figure 14. DNA damaging effect and ROS production by treatment with compounds **8** or **9**. DNA damaging effect was examined by Histone 2A.X relative expression (**A**), ROS production was detected according to dihydroethidium fluorescence (**B**). Both analyses were performed by flow cytometry, results are shown as the average ± s.d. of three independent experiments. Statistical evaluation was performed by two-way ANOVA followed by Dunnett's multiple comparisons test; ***: $p<0.001$. CDDP: cisplatin. The effect of compound **9** on DNA damage response (**C**). DNA damaging effect of **pcm** and compound **9** was evaluated by Western immunoblotting; MCF-7 cells were pre-treated with 10 μM of **pcm** or compound **9** for 30 min and exposed to UV irradiation (10 J/m^2) in the following 1 hour to induce DNA damage response. Protoapigenone (10 μM) was the positive control. Data represent the mean ± SD from three independent experiments; *: $p<0.05$, **: $p<0.01$.

Compound **9** acted as a potent modulator of DNA damage response through the inhibition of Chk1-S345 phosphorylation, while the starting material methyl *p*-coumarate (**pcm**) proved to be completely inactive in this assay (Figure 14C). This result demonstrated that compound **9** has an ability to specifically target cancer cells with high levels of endogenous DNA damage. Furthermore, compound **9** can increase Chk2-T68 phosphorylation (Figure 14C). This work was performed in collaboration with the group of Prof. Hui-Chun Wang (Kaohsiung Medical University, Kaohsiung, Taiwan).

4.6.4 In vitro cytotoxic activity of the dearomatized *p*-coumaric acid ester derivatives

The prepared and purified *p*-quinols (**9-12**) and their *O*-alkyl analogues (**13-20**) were tested for their *in vitro* cytotoxic activity on the above-described mouse lymphoma cell line pair

(L5178, L5178$_{B1}$) and on a set of human gynecological cancer cell lines (HeLa, SiHa, MCF-7, MDA-MB-231) as preliminary experiment. The currently available results of this bioassay are presented in Table 1.

Table 1. In vitro cytotoxic activity of the *p*-quinol (**9-12**) and *O*-alkyl analogues (**13-20**) of hydroxycinnamic acid esters. Results were calculated from at least 3 replicates, 95% CI: 95 % confidence interval of the mean.

	IC$_{50}$ (95% CI) (μM)					
	L5178	**L5178$_{B1}$**	**HeLa**	**SiHa**	**MCF-7**	**MDA-MB-231**
2	**58.22** (49.74 to 68.15)	**56.65** (51.11 to 62.79)	n.a.	n.a.	n.a.	n.a.
3	**71.59** (66.57 to 76.98)	**72.26** (60.63 to 86.13)	n.a.	n.a.	n.a.	n.a.
4	**44.06** (36.04 to 53.87)	**47.75** (42.69 to 53.41)	n.a.	n.a.	n.a.	n.a.
9	**0.40** (0.38 to 0.42)	**0.61** (0.57 to 0.64)	**5.6** (4.3 to 7.1)	**4.8** (4.2 to 5.4)	**4.4** (4.0 to 4.8)	**2.9** (2.7 to 3.1)
10	n.a.	**2.46** (2.24 to 2.70)	**18.5** (1.6 to 21.8)	**5.0** (4.0 to 6.3)	**4.7** (4.1 to 5.4)	**4.0** (3.5 to 4.6)
11	**21.09** (17.38 to 25.58)	**34.4** (30.66 to 38.59)	**5.7** (4.2 to 7.8)	~ **2.6**	**3.3** (3.0 to 3.5)	**1.7** (1.5 to 1.9)
12	**0.60** (0.54 to 0.68)	**1.13** (1.04 to 1.22)	**13.9** (7.9 to 24.7)	**4.2** (3.7 to 4.7)	**3.5** (3.2 to 3.7)	**2.6** (2.1 to 3.1)
13	**57.23** (52.32 to 62.60)	**54.27** (48.36 to 60.90)	**23.25** (±1.07)	**33.03** (±1.04)	**31.32** (±1.05)	n.a.
14	**35.61** (33.14 to 38.27)	**49.25** (45.37 to 53.46)	**23.98** (±1.12)	**47.38** (±1.06)	**20.28** (±1.05)	n.a.
15	**57.43** (50.24 to 65.65)	**47.26** (39.73 to 56.23)	~ **17.8**	~ **9.7**	**9.6** (8.9 to 10.4)	**5.9** (5.0 to 6.9)
16	**44.16** (37.05 to 52.63)	**40.06** (29.75 to 53.94)	n.a.	n.a.	n.a.	n.a.
17	**64.50** (57.62 to 72.21)	**41.95** (36.94 to 47.64)	**13.1** (8.1 to 21.0)	~ **7.8**	**9.8** (8.7 to 11.1)	~ **4.4**
18	**60.18** (50.06 to 72.33)	**58.30** (48.43 to 70.19)	**8.6** (7.1 to 10.4)	~ **8.4**	**8.4** (7.5 to 9.3)	**4.7** (2.6 to 8.3)
19	**63.24** (55.52 to 72.04)	**48.55** (42.47 to 55.51)	~ **10.7**	~ **9.0**	**9.7** (9.0 to 10.5)	**5.5** (3.9 to 7.6)
20	**18.25** (15.45 to 21.56)	**29.63** (26.15 to 33.57)	n.a.	n.a.	n.a.	n.a.

~: Preliminary results with ambiguous fitting; no confidence interval available; n.a.: results not yet available.

Compound **12** showed strong inhibitory activity on the mouse lymphoma cell line pair, similarly to compound **9**. The *p*-quinol analogues (**9-12**) exhibited potent cytotoxic activity on the tested human cancer cell lines, especially on MDA-MB-231 and MCF-7. This work was performed in collaboration with the group of Prof. István Zupkó (University of Szeged, Szeged, Hungary).

4.6.5 Cytotoxicity testing of an oxidized metabolite of methyl caffeate

Cytotoxic activity of the purified compound **24** was tested on human gynecological cancer cell lines (HeLa, SiHa, MCF-7, MDA-MB-231), results are summarized in Table 2. This

work was performed in collaboration with the group of Prof. István Zupkó (University of Szeged, Szeged, Hungary).

Table 2. Cytotoxic activity of compound **24** in comparison with its parent compound **cm**. Cisplatin was used as positive control; results were obtained from two biological replicates, 5 replicates each (n=10); 95% C.I. refers to 95% confidence interval for the calculated IC_{50} values.

IC_{50} [95% C.I.] (μM)				
	HeLa	**SiHa**	**MCF-7**	**MDA-MB-231**
cm	450 [396.7-551.2]	> 500	175.4 [162.3-189.7]	139.3 [116.5-166.6]
24	1.1 [1.0-1.2]	> 30	1.1 [0.9-1.4]	3.9 [3.1-4.9]
cisplatin	11.7 [10.3-13.1]	13.6 [12.6-14.7]	5.2 [4.6-5.8]	25.8 [24.4-27.4]

4.7 Investigation of the formation of hydroxycinnamic acid metabolites in biorelevant environment

4.7.1 *In vitro* antitumor activity of methyl *p*-coumarate in the presence of H_2O_2

We aimed to investigate the effect of externally induced oxidative stress on the sensitivity of cells towards **pcm**. MCF-7 cells were subjected to a treatment with **pcm** in combination with H_2O_2. Results of the assay are summarized in **Table 3**.

Table 3. Interaction between **pcm** and H_2O_2 in terms of cytotoxicity on MCF-7 cells. Combination index (CI) values are given at 50, 75 and 90% of cytotoxicity (ED_{50}, ED_{75} and ED_{90}, respectively). CI_{avg}: weighted average CI value; $CI_{avg} = (CI_{50} + 2\ CI_{75} + 3\ CI_{90})/6$. CI < 1, CI = 1, and CI > 1 represent synergism, additivity and antagonism, respectively. Dm, m and r represent antilog of the x-intercept, slope and linear correlation coefficient of the median-effect plot, respectively [65].

	CI_{50}	CI_{75}	CI_{90}	Dm	m	r	CI_{avg}
2.5:1	0.79	0.60	0.45	247.66	2.109	0.985	0.556
1.25:1	0.93	0.60	0.39	250.18	3.197	0.988	0.550
0.625:1	1.06	0.68	0.44	222.79	3.610	0.974	0.623

The results demonstrate that synergism can be observed between **pcm** and H_2O_2, especially at higher rates of inhibition that are more important in view of antitumor activity [65]. It needs to be mentioned that **pcm** was found stable for at least 92 hours in a solvent containing H_2O_2. This work was performed in collaboration with the group of Prof. Hui-Chun Wang (Kaohsiung Medical University, Kaohsiung, Taiwan).

4.7.2 Cytotoxicity testing of methyl caffeate with or without the presence of *t*-BHP induced oxidative stress

Firstly, the cytotoxicity of *t*-BHP was determined by MTT assay (72 hours) on each cell line. The obtained IC_{50} values are the followings: 27.1 μM for HeLa, 23.0 μM for SiHa, 11.3

μM for MCF-7 and 7.9 μM for MDA-MB-231, respectively (n = 6), suggesting that only moderate differences can be observed in the sensitivity of the tested cell lines to the cytotoxic effect of *t*-BHP. Then a two-step combination experiment was performed, where the cells were pre-treated with *t*-BHP at 1/3 $IC_{50}^{(72h)}$ or $IC_{50}^{(72h)}$ concentrations for 24 hours, then the medium was removed, the cells were washed and treated with **cm** (**5**) in freshly added medium. After 72 hours incubation, cell viability was evaluated, and inhibitions were calculated in comparison with cell controls that were treated the same way with the difference that the second medium did not contain **cm**. Results are presented in Figure 15.

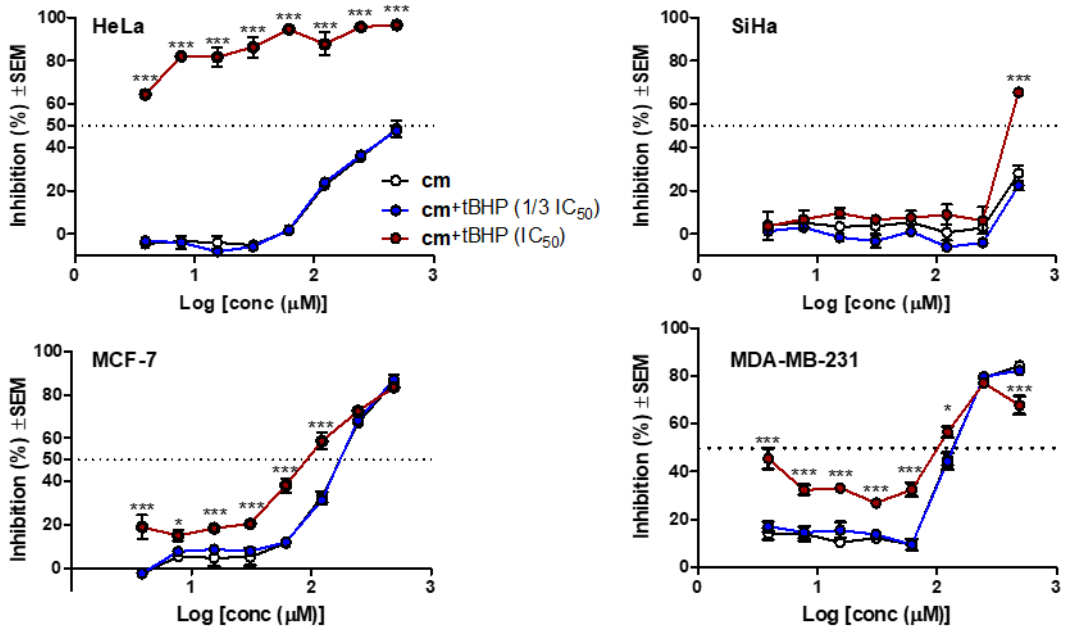

Figure 15. Cytotoxic activity of **cm** on gynecological cancer cell lines with or without *t*-BHP-induced intracellular oxidative stress. Results were analyzed by two-way ANOVA followed by a Bonferroni post-hoc test, * and ***: $p < 0.05$ and $p < 0.001$, respectively, as compared to the single treatment with **cm**; $n = 3$.

Cell lines were sensitized to the cytotoxicity of **cm** by the oxidative stress-inducing effect of *t*-BHP, except SiHa cells that are the most resistant to the activity of compound **24** as well. It is worth mentioning that the largest increase in the killing activity of **cm** was observed in HeLa cells, just like the difference between **cm** and its most active hypothesized metabolite was larger than in other cell lines. Checkerboard combination experiments were also performed by using simultaneous co-treatment with *t*-BHP and cm, and antagonism was observed in each cell line, for example 50% combination index (CI_{50}) value of 4.75 for HeLa cells, that was calculated by the Chou method [65]. This work was performed in collaboration with the group of Prof. István Zupkó (University of Szeged, Szeged, Hungary).

4.7.3 Fenton reaction of methyl *p*-coumarate

Pcm was subjected to Fenton reaction with the aim of providing possible metabolites. The effect of oxidative stress can be modeled with Fenton reaction as it can provide ˙OH radicals. After the reaction mixture was pre-purified with SPE on silica, compound **9** was detected by RP-HPLC and HPLC-MS. Figure 16 represents the HPLC-PDA chromatograms of Fenton reaction and compound **9**. This demonstrates that compound **9** may indeed be formed when **pcm** scavenges ROS.

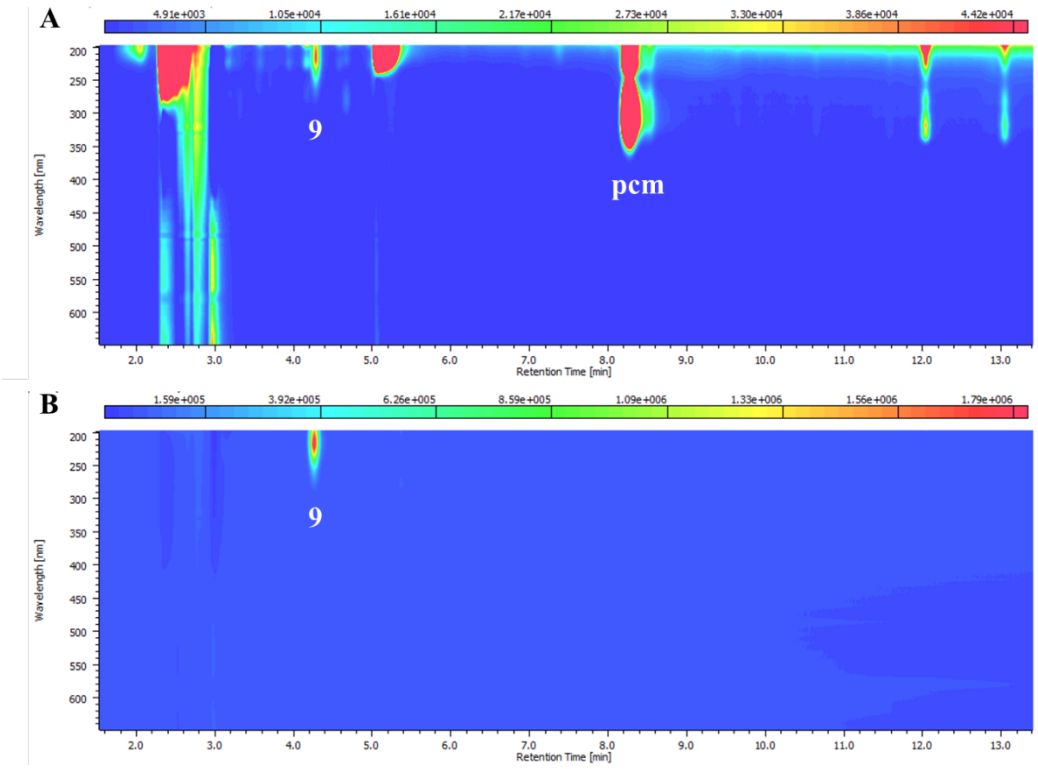

Figure 16. HPLC-PDA fingerprints of the Fenton reaction of **pcm** (**A**) and compound **9** (**B**). Colour codes respresent absorbance in µV.

4.7.4 Hydroxyl radical scavenging activity of methyl *p*-coumarate

Determination of the ˙OH radical scavenging capacity of **pcm** (**1**) was carried out by measuring the inhibiton of the oxidative damage caused to 2-deoxy-D-ribose by Fenton reaction. Trolox was used as the positive control. However **pcm** proved to be weaker (IC_{50} = 0.96 ± 0.03 mM) in this bioassay than Trolox (0.021 ± 0.002 mM), it can be still considered as an efficient ˙OH radical scavenger. **Pcm** showed similarly strong scavenging capacity as disufenton sodium (NXY-059, Cerovive), a free radical trapping antioxidant that could scavange ˙OH radicals with an IC_{50} value of 1.5 ± 0.12 mM in the same experimental setup. It is worth mentioning that NXY-059 reached phase III in clinical investigation [66]. This work

was performed in collaboration with the group of Dr. György Tibor Balogh (Gedeon Richter Plc., Budapest, Hungary).

4.7.5 *In silico* studies on the formation of methyl *p*-coumarate metabolites in the presence of ˙OH radicals

With the aim of obtaining a deeper insight into the formation of compound **9** upon ROS scavegning, *in silico* studies were performed by means of density functional theory (DFT) calculations. **Pcm** may be oxidized in two mechanical sequential chemical pathways, in the presence of highly reactive species such as ˙OH free radical. Mechanism 1 is initiated by ˙OH addition at different positions, forming radical-adducts that are stabilized by H-atom abstraction. Mechanism 2 is initiated by a H-atom abstraction, leading to the formation of a radical that undergoes ˙OH addition at various positions, resulting the corresponding adducts. Only from Mechanism 2 can be obtained compound **7**, however compound **9** can be obtained from both Mechanisms 1 and 2. Figure 17 represents the two mechanical pathways and results of the thermodinamic analysis. To allow an assessment of the role of kinetics in the formation of the products, spin density distribution for the radical intermediates was also calculated for both mechanisms; the results of these calculations are shown in Figure 18.

Since every single step exhibits negative Gibbs energies, all the predicted compounds are thermodinamically favourable with respect to **pcm** (Figure 17B). **Cm** and **pcm**-OH proved to be the most favourable compounds according to the calculated global thermodynamics (ΔG being -105.8 and 104.7 kcal.mol^{-1}, respectively), while compound **9** is much less stable (ΔG = -75.2 kcal.mol^{-1}) as a result of dearomatization. Spin density distribution of the most thermodynamically favourable radical intermediate, [**9**-OH]˙, however, suggests the unpaired electron in this species to be most likely present at position C-1′ (Figure 18B).

This work was performed in collaboration with the group of Prof. Patrick Trouillas (University of Limoges, Limoges, France).

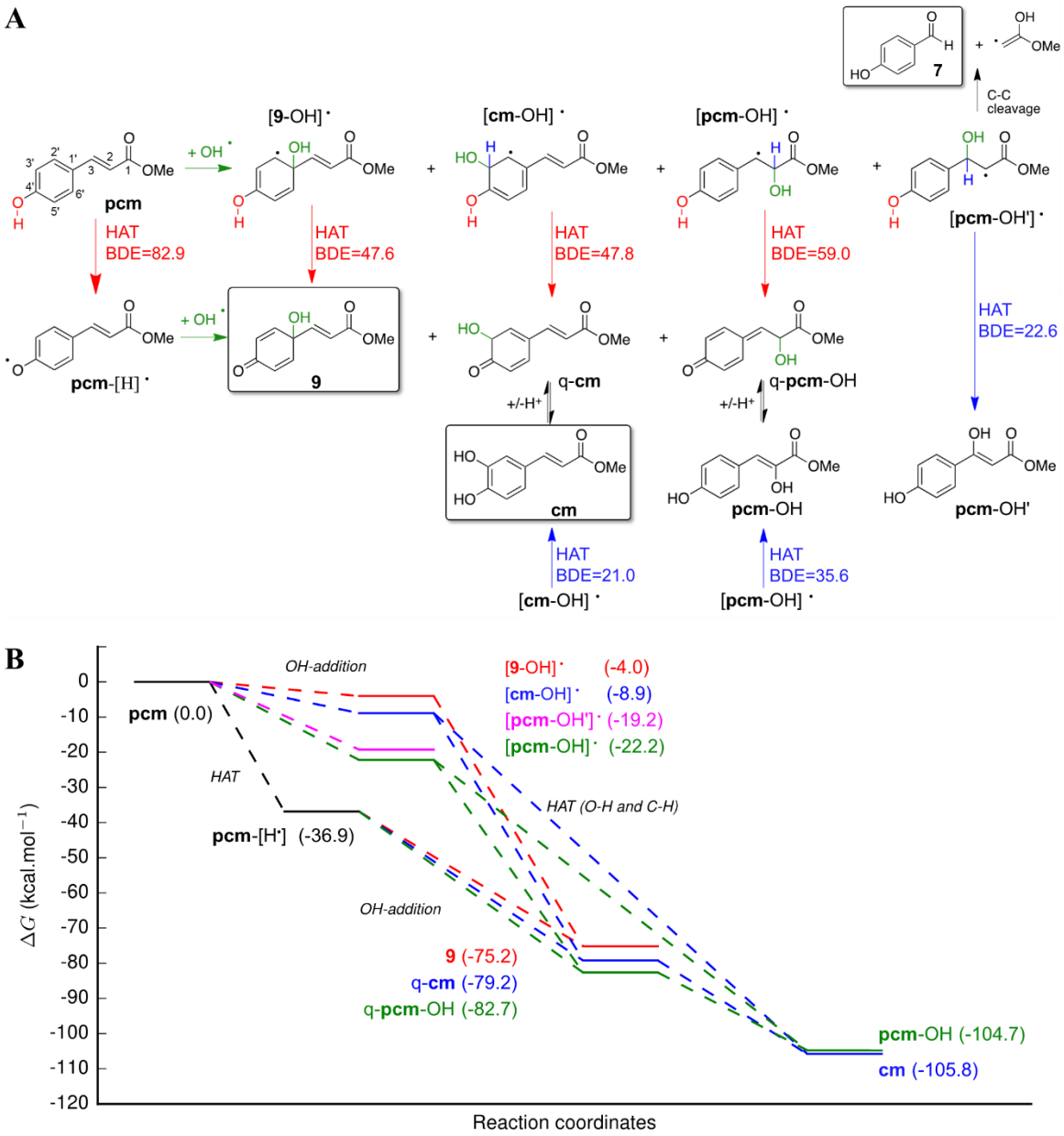

Figure 17. Reactivity of **pcm** in presence of ˙OH radical (**A**) and thermodynamics of the reaction steps (**B**). HAT: hydrogen atom transfer, q-**pcm** and q-**cm** represent quinone forms of **pcm** and **cm**, respectively. Frames mark species observed experimentally from the Fenton reaction of **pcm** and/or from its oxidation with PIFA. Bond dissociation enthalpy (BDE) is defined as the enthalpy required to the homolytic cleavage of X-H bond as follows: BDE(R-H) = *H*(R˙, 298K) + *H*(H˙, 298K) - *H*(R-H, 298K), where *H* is the enthalpy. O-H and C-H BDE values for each HAT are given in red and blue, respectively, in kcal.mol^{-1}. Gibbs energies (ΔG, kcal.mol^{-1}) are indicated for each reaction step relative to that of **pcm**.

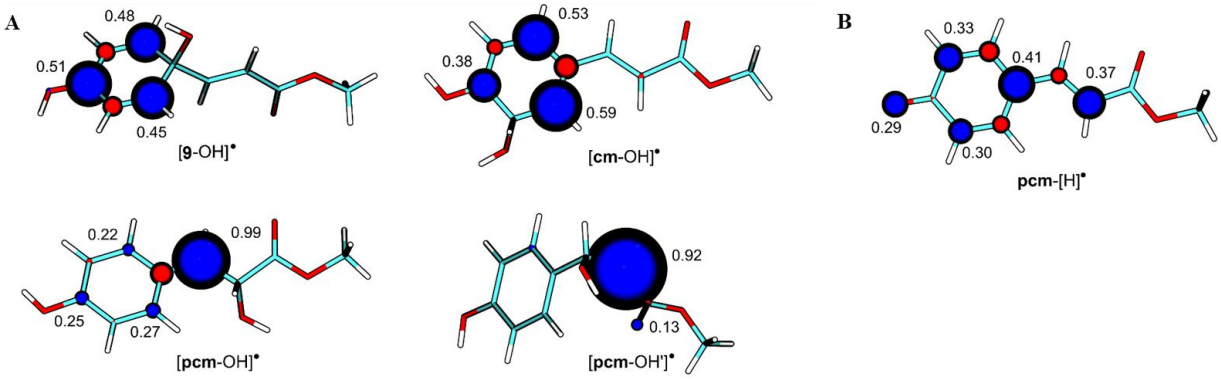

Figure 18. Spin density distribution of the radicals formed by the reaction between **pcm** and ˙OH radicals. Radicals formed through OH-addition (**A**); radical formed through hydrogen atom abstraction (**B**). Blue and red spheres illustrate positive and negative atomic spin densities, respectively.

5. DISCUSSION

5.1 Oxidative reaction of hydroxycinnamates with hypervalent iodine reagents

5.1.1 Oxidation of methyl *p*-coumarate with hypervalent iodine reagent

Our aim was to evaluate whether or not more effective compounds can be formed from methyl *p*-coumarate through free radical scavenging. To this, first we investigated the effect of various oxidative conditions on the cytotoxic activity of **pcm** (**1**). It was oxidized with a hypervalent iodine (III) reagent (PIFA) in four different solvents or solvent systems, and with pyridinium chlorochromate (PCC) in one solvent. PIFA is not a classical biomimetic oxidative reagent. Still, its ability to catalyze oxidation through single-electron transfer (SET) that leads to a cation-radical intermediate whose deprotonation may form the phenoxyl radical (i.e. the intermediate of hydrogen atom transfer; HAT reaction) [13] made it an attractive choice to initiate our studies. It is also worth mentioning that the ROS scavenging by *p*-coumaric acid was previously suggested to take place through either SET or HAT mechanism [67].

After the cytotoxic testing of the product mixtures, the most effective of them were selected to perform scale-up, and from these reactions altogether 5 metabolites were isolated and determined; their structures are presented in Figure 5, Section 4.2. Compound **6** has most likely been formed from **pcm** in a similar way to that formerly described for the dihydrobenzofurane dimers of methyl caffeate (**cm**) or methyl ferulate, followed by the elimination of a phenol group that led to the formation of the benzofurane skeleton. The formation of compound **5**, i.e. methyl caffeate, and **7**, i.e. *p*-hydroxybenzaldehyde can be explained by the impact of the oxidative environment. However, compound **8** (methyl grevillate or methyl-2,5-dihydroxycinnamate), that has been previously isolated from *Grevillea robusta* A. CUNN [68] and from *Murraya paniculata* [69], has a highly unexpected structure. It has

been described that PIFA can selectively oxidize *p*-phenols through a cationic [70] or cation-radical intermediate [71], that can suspect the subsequent formation and opening-up of an epoxide ring, explaining the unexpected migration of the hydroxyl group from para- to meta-position. Compound **9** (graviquinone) is also a natural compound that has first been isolated from *Grevillea robusta* (commonly known as "silky oak"), and described as an *in vitro* cytotoxic compound against MCF-7, NCI-H460, and SF-268 cell lines [68].

5.1.2 Preparation of synthetic analogues of compound 9

A set of antitumor 1′-*O*-alkyl protoflavone analogues were previously prepared and investigated for their structure-activity relationships by our research group. The butyl ether derivative of protoapigenone showed stronger activity against cancer cell lines (Hep3B, MCF-7 and MDA-MB-231) than protoapigenone itself [17]. Furthermore, protoflavone derivatives showed selective cytotoxicity on certain MDR cancer cell lines as compared to their drug-sensitive counterparts [72]. Considering these results and the potent antitumor effect of compound **9**, we decided to prepare further *p*-quinol analogues and their *O*-alkyl derivatives from *p*-coumaric acid esters. By adopting the chemical strategy previously used for protoflavones [73], further new p-quinols (**10**-**12**), and their 1′-*O*-butyl (**13**, **15**, **17**, **19**) and propargyl (**14**, **16**, **18**, **20**) analogues were successfully obtained.

5.2 AAPH- or peroxynitrite-induced oxidation of hydroxycinnamates

To further evaluate possible hydroxycinnamate metabolites that may be formed through ROS/RNS scavenging, we selected two model reagents: 2,2′- azobis(2-methylpropionamidine) dihydrochloride (AAPH) and peroxynitrite ($ONOO^-$). AAPH is a peroxyl radical initiator best known from its use in the *in vitro* antioxidant assay ORAC (oxygen radical absorbing capacity) [74]. Since alkyl peroxyl radicals are among the major species causing oxidative stress [13], this reagent is biomimetic. Peroxynitrite, on the other hand, is a well-known biological oxidant itself, which can cross biological membranes and diffuse across up to two cell diameters, and despite its short half-life, it may be scavenged by small-molecule antioxidants [75]. This reagent is therefore not only biomimetic, but also fully biorelevant.

5.2.1 In situ continuous-flow biomimetic reaction of methyl *p*-coumarate with peroxynitrite

A continuous flow reaction (CFR) system was applied, in which $ONOO^-$ can be prepared in situ from nitrite and hydrogen peroxide similarly to the way described by Robinson and Beckman [76]. By using this approach, the in situ prepared $ONOO^-$ could be promptly reacted with methyl *p*-coumarate (**pcm**). The structures of the isolated four compounds (**7** and **21-23**)

are presented in Figure 8 in Section 4.4.1. Compound **22** was prepared in this work as a new compound.

In this reaction of **pcm**, *p*-hydroxybenzaldehyde (**7**) was also observed, similarly to its reaction with PIFA or $OH^{\bullet}$ radicals (see Section 4.2 and 4.7.5). The formation of *p*-nitrophenol (**21**) would be explained by a similar fragmentation and subsequent radical reaction of the aromatic ring with $ONOO^-$. Compound **22**, that is an unexpected product, must be formed in a secondary reaction of a reactive intermediate of **pcm**, oxidized at the trans-olefin moiety, and with a chloride ion that comes from HCl that is used in the first step to prepare peroxynitrous acid and it remains in the solution as NaCl after the subsequent addition of NaOH. Although this may be considered as a contamination, chloride ion is a major electrolyte present in the intra- and extracellular fluid, therefore its presence further strengthens the notion that our experimental setup is appropriate to obtain metabolites that may possibly be formed through $ONOO^-$ scavenging in a biological environment. $ONOO^-$ plays an important role in the nitration of biological macromelcules in redox signaling (mainly through nitrolipids) and oxidative damage (mainly through nitroproteins) [77]. Therefore, similarly to the case of compound **21**, the formation of compound **23** represents an irreversible structural change through nitration that may also take place when a small-molecule antioxidant, such as **pcm** scavenges $ONOO^-$.

5.2.2 Longitudinal study and bioactivity-guided isolation of AAPH or peroxynitrite-oxidized metabolites of methyl caffeate

Our aim was to find ROS/RNS scavenging-related oxidized bioactive metabolites from the reaction between **pcm** (**1**) or **cm** (**5**) and $ONOO^-$ or AAPH. As the prepared reaction mixtures were tested for their cytotoxicity on human gynecological cancer cell lines (HeLa, SiHa, MCF-7 and MDA-MB-231), none of the product mixtures of **pcm** was found to be active. In contrast to this, a highly increased cytotoxic activity was observed in the case of an AAPH-oxidized reaction mixture of **cm**, and this was the strongest on HeLa cells. Subsequently, this reaction was carried out as a longitudinal study, and the best reaction time for scale-up (24 h) was selected, when the product profile seemed to be the most favorable and the cytotoxic effect was the highest. The increased cytotoxic activity on HeLa cells was in good correlation with the amounts of compound **24** present in the samples (Figure 9C). Of the scaled-up reaction, performing a bioactivity-guided purification strategy, compound **24** was isolated. From an other, not cytotoxic fraction, compound **25** was isolated as a major product. It needs to be hightlighted that compound **24** was also present in the product mixture obtained from the reaction between **cm** and peroxynitrite (see Figure 11. in Section 4.4.4). As peroxynitrite is an

abundant oxidant in various tissues, and it has critital role in redox signaling, oxidative stress and thereby in the pathomechanism and progression of several diseases [78], [79], it is an interesting observation that compound **24**, a potent antitumor compound formed from a dietary antioxidant (**cm**) upon scavenging this reactive nitrogen species.

5.3 Biological activity of the obtained metabolites

5.3.1 Antitumor potential of the oxidized methyl *p*-coumarate derivatives

***In vitro* cytotoxicity**

As it is described above (see Section 4.6.1), methyl *p*-coumarate (**pcm**) and its oxidized derivatives (**5-9**) were tested for their cytotoxic activity first on a mouse lymphoma cell line pair (L5178 and $L5178_{B1}$). The MDR sub-cell line was obtained of L5178 by transfection with the human *ABCB1* gene, therefore it is a good model of a major resistance mechanism, drug efflux by the ABCB1 transporter commonly referred to as P-glycoprotein or Pgp. Overcoming this resistance mechanism is a persisting challenge in cancer research [80], [81]. Compounds **8** and **9** were also tested on a human cancer cell line panel (MCF-7, HeLa, SiHa, A549, NCI-H661, NCI-H460 and NCI-H460/R). The parent antioxidant **pcm** showed very low cytotoxic activity, while some of its oxidized metabolites exerted *ca*. 2-3 orders of magnitude stronger cytotoxicity. The doxorubicin NCI-H460/R cell line showed nearly 10-fold cross resistance to **pcm**, as compared to the NCI-H460 parental cell line. In case of the oxidized metabolites, a 2.4 times cross-resistance was observed in the MDR cell line $L5178_{B1}$ towards the hydroquinone analogue (**8**), which may imply this compound as a likely substrate of the ABCB1 efflux transporter. In comparison with **pcm**, the resistance profile to compound **8** was much more favourable in the NCI-H460/-H460/R cell line pair, exhibiting a less than twice cross-resistance in the MDR one. Compound **9**, on the other hand, was able to fully bypass resistance of both the ABCB1-transfected cell line and the NCI-H460/R cell line adapted to doxorubicin. This compound showed similarly strong activity as the positive control doxorubicin on L5178 cell line. At the same time, it was 28.9 times stronger than that on the resistant $L5178_{B1}$ cell line, thanks to bypassing efflux-mediated resistance. Further, compound **9** also demonstrated a good selectivity towards cancer cells, as shown by the nearly 10-times selective cytotoxicity against the lymphoma cell lines, and a *ca*. 2-3 times selectivity against the NCI-H460 and NCI-H661 cell lines, in comparison with the immortalized human keratinocytes (HaCaT).

Cell death analysis

The percentages of apoptotic, necrotic and viable cells were determined in human lung carcinoma cell lines (NCI-H460, NCI-H460/R, A549 and NCI-H661) and in normal human

keratinocytes (HaCaT), after treatment with compound **8** or **9**. Both of the compounds induced cellular necrosis in this experiment. Compound **8** produced the strongest effect on NCI-H460 cells, in accordance with the cytotoxicity assay, in which this cell line was found to be the most sensitive to compound **8**. It must be highlighted, that compound **9** increased the percentage of necrotic NCI-H661 cells from 2.58 % (untreated control) to 44.82 % (treated). In our previous study, a similar effect was observed for a *p*-quinol flavonoid, protoapigenone that also induced necrosis-type cell death in association with ATR inhibition through Chk1 phosphorilation, leading to the accumulation of DNA lesions [54]. Considering this and the structural relationship between compound **9** and protoapigenone, both containing the same *p*-quinol pharmacophore, we aimed to investigate its potential ability to exert DNA damage and interfere with DNA damage response at the same time.

DNA damage studies

As histone H2A.X is a well-known marker of DNA damage causing double-strand breaks (DSBs) [82], its expression was analysed following treatment with compound **8** or **9** (see Section 4.6.3). DNA damage was induced by compound **9** in NCI-H460 and NCI-H460/R cells with a significantly increased expression of H2A.X, but it was decreased in normal HaCaT cells after treated with compound **9**, suggesting its selectivity towards DNA damaging in cancer cells. Compound **8** reduced the expression of H2A.X in most of the cancer cells and also in HaCaT cells, indicating its DNA protective effect (Figure 14A). After treatment with compound **9**, a significant increase of ROS levels was observed in A549, NCI-H460 and NCI-H661 cells, however it was decreased in NCI-H460/R and HaCaT cells, that also demonstrates the selectivity of compound **9** towards cancer cells. The opposite effect on NCI-H460/R cells as compared to that on NCI-H460 cells should be discussed considering the lower antioxidant potential of the resistant cell line, comparing with the parental cell line [83]. On the other hand, compound **8** decreased ROS levels in all tested cancer cell lines and also in HaCaT cells (Figure 14B). These results suggest different mechanisms of action for compounds **8** and **9**.

While the starting material **pcm** (**1**) was completely inactive in this assay, compound **9** acted as a potent modulator of DNA damage response through the inhibition of Chk1-S345 phosphorylation (see Figure 14C in Section 4.6.3). The serine-threonine checkpoint kinases 1 and 2 (Chk1 and 2) play a key role in the DNA damage signalling response. Chk1 is activated through phosphorylation by the ataxia telangiectasia and Rad3-related kinase (ATR), and Chk2 is activated by the ataxia telangiectasia mutated kinase (ATM). It has been shown that tumour cells whose DNA repairing is defective, accumulate high levels of DNA damage. Chk1 is

important for the stability of stalled replication forks [84]. Small molecules that can inhibit Chk1 are potential therapeutic agents against specific cancers such as Fanconi Anemia (FA) pathway deficient tumors [85]. It needs to be highlighted that the sensitivity to Chk1 inhibition is associated with replication stress in many cancers, for example neuroblastoma or metastatic melanoma, in which there is a high expression of Chk1 mRNA [86], [87]. Consequently, our results suggest that compound **9**, as a Chk1 inhibitor has a potential to specifically target cancer cells that have high levels of endogenous DNA damage. It is well-known that the increased expression of phosphorylated H2A.X is a marker of DNA double strand breaks (DSBs) [82], and our results showed that treatment with compound **9** significantly increased the expression of H2AX in cancer cells (Figure 14A). DSBs can be responsible for the ATM activation, as ATM dependent phosphorylation is also correlated with the phosphorylation of H2A.X. According to our results, compound **9** can increase Chk2-T68 phosphorylation, suggesting that it could induce DSBs and therefore activate the ATM-Chk2 pathway. This was different to the positive control protoapigenone, which did not influence the ATM-dependent phosphorylation of Chk2 in accordance with the previous results of our research group [54].

5.3.2 Antitumor potential of the synthetic analogues of compound 9

The prepared and determined *p*-quinols (**9-12**) and their butyl- (**13, 15, 17, 19**) and propargyl-ether (**14, 16, 18, 20**) analogues were tested for their cytotoxic activity on a sensitive (L5178) and a multi-drug resistant ($L5178_{B1}$) mouse lymphoma cell line, and on a set of human gynecological cancer cell lines. The *p*-quinol analogue (**12**) of *p*-coumaric acid isopropyl ester showed similarly strong cytotoxic activity as compound **9** on the mouse lymphoma cell line pair. The resistance profile of the butyl ether analogues were better on the mouse lymphoma cell line pair in comparison with that of the propargyl-ether analogues. The *p*-quinol analogues showed stronger cytotoxic activity on all the tested cancer cell lines then the *O*-alkyl analogues, suggesting that substitution decreasing the cytotoxic potential.

5.3.3 Antitumor potential of the oxidized methyl caffeate derivatives

Cell viability testing

The purified compound **24** was tested for its cytotoxicity on a panel of human gynecological cancer cell lines (HeLa, SiHa, MCF-7, MDA-MB-231). For the results see Section 4.6.5.

Polyphenolic compounds can react with constituents of cell culture media to generate H_2O_2 and degradation products that may produce bioactivites erroneously attributed to the polyphenol [88], but in this case it may be of little importance. As compound **24** has a catechol

group, it may be considered as an antioxidant, somewhat similarly to the non-cytotoxic methyl caffeate (**cm**). The pharmacological value of compound **24** is well established, as its antitumor properties have been thoroughly studied by other research groups both *in vitro* and *in vivo* [46]. Compound **24** was previously reported to have a potent antiangiogenic activity [44] and *in vivo* antimetastatic activity by increasing IL-25 secretion from tumor-associated fibroblasts [46], suggesting that compound **24** is a promising lead for further clinical development. It is a very interesting finding that this compound was present not only when methyl caffeate (**cm**) was reacted with AAPH, but also from its reaction with peroxynitrite (see Section 4.4.4), a fully biorelevant reactive nitrogen species that plays a major role in oxidative stress.

5.4 Investigation of the formation of hydroxycinnamic acid derivatives in biorelevant environment

In vitro cytotoxic activity of methyl *p*-coumarate in the presence of H_2O_2-induced oxidative stress

Our aim was to investigate the externally provoked oxidative stress on the sensitivity of cells towards **pcm** (**1**). MCF-7 cells were subjected to a combined treatment with **pcm** in combination with H_2O_2 (see Section 4.7.1). The results clearly demonstrate that synergism can be observed between **pcm** and H_2O_2, especially at higher rates of inhibition. Furthermore, a tendency can be observed in favour of higher H_2O_2 *vs*. **pcm** ratios, that further strengthens the correlation between the formation of oxidized **pcm** metabolites and the level of oxidative stress. It needs to be highlighted that **pcm** was found stable for at least 92 hours dissolved in methanol containing H_2O_2, indicating that the observed increase in the cytotoxic activity is unlikely to come from a simple chemical reaction between H_2O_2 and **pcm**.

The effect of the presence of *t*-BHP induced oxidative stress on the cytotoxicity of methyl caffeate

With this experiment, we aimed to evaluate whether a possible oxidative stress-related intracellular in situ formation of compound **24** (and other possible bioactive metabolites) from **cm** has the chance to modulate the observed cytotoxic effect. *Tert*-butyl hydroperoxyde (*t*-BHP) is a well-known lipophilic inducer of intracellular oxidative stress [89]. First, the cytotoxicity of *t*-BHP was determined on different cancer cell lines, showing only moderate differences in their sensitivity. According to a recent longitudinal study, *t*-BHP was able to induce significant levels of oxidative stress in MCF-7 cells in 24-hours treatment [89]. Considering this, and to prevent a possible chemical reaction between *t*-BHP and **cm** that could be catalyzed by constituents of cell culture medium [88], a two-step combination experiment was performed

(see Section 4.7.2). This was an update to our first experimental setup using H_2O_2 and **pcm** as a simple co-treatment (see Section 4.7.1), aiming to further increase the biological relevance of our results. We found that the tested cell lines were sensitized to the cytotoxic effect of **cm** by the oxidative stress induced by *t*-BHP, with the sole exception of SiHa cells that were also the most resistant to compound **24**. Furthermore, the largest increase in the killing activity of **cm** was observed in HeLa cells, and even the difference between **cm** and its most active hypothesized metabolite was larger in this cell line than in others. The pre-treatment with *t*-BHP at lower concentration did not exert any significant change in the killing activity of **cm** on any of the cell lines, therefore it is unlikely to experience an artefact due to the reaction between remanining traces of extracellular *t*-BHP and **cm**. This was also confirmed by checkerboard combination experiments, in which simultaneous co-treatment was performed with *t*-BHP and **cm**, revealing antagonism in each cell line. The increased efficiency of **cm** in such conditions could certainly be due to many reasons; the alleged formation of bioactive metabolites is one possibility. The case of the MDA-MB-231 cells (Figure 15. in Section 4.7.2) well demonstrates this complex situation; the cytotoxicity of **cm** on the cells highly exposed to oxidative stress could not be described with a single sigmoidal dose-response curve, in contrast with the case of the single treatment. We attempted to carry out HLPC-MS/MS studies on lysates of cells pre-treated a similar way, however no conclusive results were obtained. Therefore, a direct evidence to the biological relevance of a transformation of **cm** to compound **24** induced by ROS/RNS scavenging, is currently not available.

Fenton reaction

Since the biomimetic nature of PIFA-catalized oxidation of **pcm** to compound **9** may be debated, we performed the Fenton reaction of **pcm** to evaluate its behaviour in a more appropriate chemical model of oxidative stress, i.e. the presence of excess $^{\bullet}$OH radicals. The qualitative metabolite fingerprint obtained in such an experimental setup provides valuable information on what compounds may be formed when ROS scavenging by **pcm** takes place. Our results clearly demonstrate that compound **9** is among these possible metabolites; see Figure 16 in Section 4.7.3. However, it must be noted that the conditions of such an extreme oxidative environment do not allow to draw any further quantitative conclusion as to what rate such transformations may take place in a biological environment.

$^{\bullet}$OH radical scavenging activity

Methyl *p*-coumarate (**pcm**) is a diatery antioxidant that has been shown to prevent lipid peroxidation in rat liver microsomes with an IC_{50} value of 0.4 μM [90]. The *in vitro* antioxidant

activity of *p*-coumaric acid is well described, it was shown to have a potent DPPH, ABTS, superoxide anion radical and H_2O_2 scavenging activity, it can reduce ferric ions (Fe^{3+}) and chelate ferrous ions (Fe^{2+}), and it inhibits lipid peroxidation [91]. Similar effects were expected from **pcm**, as the ester function is unlikely to interfere with these antioxidant mechanisms. We studied the •OH radical scavenging activity of **pcm**, to investigate whether the identified bioactive metabolites form from **pcm** upon ROS scavenging.

***In silico* studies**

With the aim of getting a deeper insight into the possibility of the formation of compound **9** upon ROS scavenging, *in silico* studies were performed by means of DFT calculations. In the presence of highly reactive oxygen species such as •OH radical, methyl *p*-coumarate may be oxidized in two distinct mechanical chemical pathyways, that are detailed in Section 4.7.5. Interestingly, only compound **9**, **cm** and compound **7** could be experimentally identified among those that can be formed through these mechanisms, suggesting the importance of kinetics to allow the formation of thermodynamically less favourable metabolites like compound **9**. A competition can be observed between Mechanism 1 and 2, in other words between H-atom abstraction and OH-addition to **pcm**. The major pathway likely starts with H-atom abstraction, as it is more favourable from the *p*-OH, explaining the experimental formation of **cm** and compound **9**. **Cm** is the global thermodynamic product, while compound **9** is a kinetic product from the OH-addition step that is favoured by the most likely localization of the unpaired electron in the phenoxyl radical species (Figure 17 in Section 4.7.5). The observation of compound **7** in this experiment as a product also emphasizes the important role of kinetics. Further, even though **cm** was found to be the major product by theoretical calculations, it has only been experimentally observed from the oxidation with PIFA and not from the Fenton-reaction of **pcm**. This latter is likely a false negative result, since the catechol moiety of **cm** should make it sensitive to further oxidation, therefore its rapid decomposition and consequential difficulties of detection can occur during Fenton-reaction. The formation of the unexpected hydroquinone compound **8** is a result of the migration of the *p*-hydroxyl group, to which the only likely explanation seems to be the formation of an epoxide intermediate and subsequent ring opening.

6. SUMMARY

The main aims of the Ph.D. work presented in this dissertation was to prepare oxidized metabolites of hydroxycinnamates with different oxidizing agents, study their potential

antitumor activites, and to investigate their possible formation upon ROS/RNS scavenging. Our results may be summarized as follows:

1. Preparation of semi-synthetic oxidized cinnamic acid derivatives. In the performed different oxidative reactions, altogether 21 oxidized hydroxycinnamic acid derivatives were prepared and isolated by combined chromatographic techniques. Various oxidizing agents were used, such as hypervalent iodine reagents (PIFA, PIDA), a biorelevant reactive nitrogen species, peroxynitrite, and a peroxyl radical initiator, AAPH. The twenty-one oxidized compounds were obtained from the following chemical approaches:

- Five compounds (**5**-**9**) from the diversity-oriented oxidation of methyl *p*-coumarate (**pcm**) with hypervalent iodine reagents,
- Eleven compounds (**10**-**20**) from the oxidative dearomatization of different *p*-coumaric acid esters with hypervalent iodine reagents,
- Four compounds (**7**, **21**-**23**) from the oxidation of methyl *p*-coumarate (**pcm**) with peroxynitrite in a continuous-flow reaction system,
- Two compounds (**24**, **25**) from the oxidation of methyl caffate (**cm**) with AAPH.

Compound **7**, *p*-hydroxy-benzaldehyde was obtained from the oxidation of methyl *p*-coumarate with two different oxidants.

Among the 21 compounds prepared during this work, 11 compounds (**10**-**20**) were obtained as new compounds.

2. Biological evaluation of the isolated oxidized hydroxycinnamic acid derivatives. The following results were achieved in research collaboration:

- From the oxidation of methyl *p*-coumarate (**pcm**) with hypervalent iodine reagents, two metabolites with potent antitumor effect were identified, compounds **8** and **9**. In particular, compound **9** (graviquinone) showed *in vitro* antitumor activity 2-3 orders stronger than **pcm**, and it bypassed multi-drug resistance mediated by the ABCB1 transporter and by all the mechanisms present in a non-small cell lung carcinoma cell line adapted to doxorubicin. Further, compound **9** demonstrated favourable tumour selectivity; it induced DNA damage in lung carcinoma cells while exerting DNA protecting activity in normal human keratinocytes, and modulated DNA damage responses in MCF-7 cells.
- Preliminary bioactivity studies on the synthetic analogues of compound **9** suggest that the several of the 1′-*O*-alkyl ethers of related hydroxycinnamate derivatives are also

promising antitumor compounds, and that they have very different cell line specificity as compared to compound **9**.

- From the oxidation of methyl caffeate (**cm**) with AAPH or peroxynitrite, a highly potent antitumor compound (**24**), a dimerization product was identified.

3. Investigation of the formation of hydroxycinnamic acid metabolites in biorelevant environment. Our results support the possibility of the oxidative stress-related formation of the identified bioactive oxidized hydroxycinnamate metabolites, as follows:

- In a combination treatment of MCF-7 cells with **pcm** and H_2O_2, synergism was observed, i.e. the *in vitro* antitumor activity of **pcm** was significantly increased in the presence of H_2O_2-induced oxidative stress.
- The H_2O_2-induced oxidative stress-related formation of compound **9** from **pcm** was confirmed by Fenton reaction. *In silico* calculations performed in research collaboration suggest compound **9** as a kinetic product of **pcm** upon $^{\bullet}OH$ radical scavenging, while methyl caffeate (**cm**) as the thermodynamic product.
- Compound **24** was formed from **cm** under biomimimetic oxidative conditions, showing that it inevitably takes place when **cm** scavenges peroxyl radicals or peroxynitrite.
- The presence of *t*-BHP pre-treatment-induced oxidative stress increased the cytotoxic activity of **cm** in a way that the change of activity in different cell lines coincided with the cells' sensitivity to the identified active metabolite compound **24**. Co-treatment of the cells with *t*-BHP and **cm** at the same time, however, demonstrated antagonism, suggesting that the increased cytotoxicity was due to the induced oxidative stress and not because of a cell culture medium-catalyzed chemical reaction between *t*-BHP and **cm**.

Altogether, our results on hydroxycinnamates suggest that an oxidative stress-related in situ formation of new bioactive metabolites from antioxidants is possible in biological environments. Through identifying compounds **9** and **24** as valuable antitumor agents it was also shown that this phenomenon can be used as the basis of discovering new bioactive compounds through diversity-oriented oxidative transformations of small molecule antioxidants.

REFERENCES

[1] R. Merkl, I. Hrádková, V. Filip, J. Šmidrkal, Antimicrobial and antioxidant properties of phenolic acids alkyl esters, *Czech Journal of Food Sciences*, vol. 28, no. 4, pp. 275–279. **2010**

[2] D.H. Hahn, J.M. Faubion, L.W. Rooney, Sorghum phenolic acids, their high performance liquid chromatography separation and their relation to fungal resistance, *Cereal chemistry.*, vol. 60, no. 4, pp. 255–259. **1983**

[3] S. Khadem, R.J. Marles, Monocyclic phenolic acids; hydroxy- and polyhydroxybenzoic acids: occurrence and recent bioactivity studies, *Molecules*, vol. 15, no. 11, pp. 7985–8005. **2010**

[4] K.R. Martin, C.L. Appel, Polyphenols as dietary supplements: A double-edged sword, *Nutrition and Dietary Supplements*, no. 2, pp. 1-12. **2009**

[5] H.R. El-Seedi, A.M.A. El-Said, S.A.M. Khalifa, U. Göransson, L. Bohlin, A.K. Borg-Karlson, R. Verpoorte, Biosynthesis, natural sources, dietary intake, pharmacokinetic properties, and biological activities of hydroxycinnamic acids, *J. Agric. Food Chem.*, vol. 60, no. 44, pp. 10877–10895. **2012**

[6] K. Herrmann, Occurrence and content of hydroxycinnamic and hydroxybenzoic acid compounds in foods, *Crit Rev Food Sci Nutr*, vol. 28, no. 4, pp. 315–347. **1989**

[7] N. Razzaghi-Asl, J. Garrido, H. Khazraei, F. Borges, O. Firuzi, Antioxidant properties of hydroxycinnamic acids: a review of structure- activity relationships, *Curr. Med. Chem.*, vol. 20, no. 36, pp. 4436–4450. **2013**

[8] K.M. Herrmann and L.M. Weaver, The shikimate pathway, *Annual Review of Plant Physiology and Plant Molecular Biology*, vol. 50, no. 1, pp. 473–503. **1999**

[9] D. Huang, Dietary Antioxidants and Health Promotion, *Antioxidants*, vol. 7, no. 1, Art. no. 1, **2018**

[10] H.E. Billingsley, S. Carbone, The antioxidant potential of the Mediterranean diet in patients at high cardiovascular risk: an in-depth review of the PREDIMED, *Nutrition & Diabetes*, vol. 8, no. 1, Art. no. 1. **2018**

[11] S.K. Chang, C. Alasalvar, F. Shahidi, Superfruits: Phytochemicals, antioxidant efficacies, and health effects – A comprehensive review, *Critical Reviews in Food Science and Nutrition*, vol. 59, no. 10, pp. 1580–1604. **2019**

[12] S.B. Nimse, D. Pal, Free radicals, natural antioxidants, and their reaction mechanisms, *RSC Adv.*, vol. 5, no. 35, pp. 27986–28006. **2015**

[13] A. Hunyadi, The mechanism(s) of action of antioxidants: From scavenging reactive oxygen/nitrogen species to redox signaling and the generation of bioactive secondary metabolites, *Med Res Rev*, vol. 39, no. 6, pp. 2505–2533. **2019**

[14] J.J. Bozell, B.R. Hames, D.R. Dimmel, Cobalt-Schiff base complex catalyzed oxidation of para-substituted phenolics. Preparation of benzoquinones, *J. Org. Chem.*, vol. 60, no. 8, pp. 2398–2404. **1995**

[15] Y. Shingai, A. Fujimoto, M. Nakamura, T. Masuda, Structure and function of the oxidation products of polyphenols and identification of potent lipoxygenase inhibitors from Fe-catalyzed oxidation of resveratrol, *J Agric Food Chem*, vol. 59, no. 15, pp. 8180–8186. **2011**

[16] L. Pieters, S. Van Dyck, M. Gao, R. Bai, E. Hamel, A. Vlietinck, G. Lemiére, Synthesis and biological evaluation of dihydrobenzofuran lignans and related compounds as potential antitumor agents that inhibit tubulin polymerization, *J. Med. Chem.*, vol. 42, no. 26, pp. 5475–5481. **1999**

[17] A. Hunyadi, D.-W. Chuang, B. Dankó, M.Y. Chiang, C.-L. Lee, H.-C. Wang, C.-C. Wu, F.-R. Chang, Y.-C. Wu, Direct semi-synthesis of the anticancer lead-drug protoapigenone from apigenin, and synthesis of further new cytotoxic protoflavone derivatives, *PLoS One*, vol. 6, no. 8, 1-10. **2011**

[18] M. Sova, Antioxidant and antimicrobial activities of cinnamic acid derivatives, *Mini Rev Med Chem*, vol. 12, no. 8, pp. 749–767. **2012**

[19] D. Szwajgier, J. Pielecki, Z. Targoński, Antioxidant activities of cinnamic and benzoic acid derivatives, *Acta Scientiarum Polonorum Technologia Alimentaria*, vol. 4, no. 2, pp. 129–142. **2005**

[20] E. Graf, Antioxidant potential of ferulic acid, *Free Radic. Biol. Med.*, vol. 13, no. 4, pp. 435–448. **1992**

[21] S. Foley, S. Navaratnam, D.J. McGarvey, E.J. Land, T.G. Truscott, C.A. Rice-Evans, Singlet oxygen quenching and the redox properties of hydroxycinnamic acids, *Free Radic. Biol. Med.*, vol. 26, no. 9–10, pp. 1202–1208. **1999**

[22] O. Firuzi, L. Giansanti, R. Vento, C. Seibert, R. Petrucci, G. Marruso, R. Agostino, L. Saso, Hypochlorite scavenging activity of hydroxycinnamic acids evaluated by a rapid microplate method based on the measurement of chloramines, *Journal of Pharmacy and Pharmacology*, vol. 55, no. 7, pp. 1021–1027. **2003**

[23] J. Laranjinha, O. Vierira, L. Almeida, V. Madeira, Inhibition of metmyoglobin/H2O2-dependent low density lipoprotein lipid peroxidation by naturally occurring phenolic acids, *Biochem. Pharmacol.*, vol. 51, no. 4, pp. 395–402. **1996**

[24] C. Siquet, F. Paiva-Martins, J.L.F.C. Lima, S. Reis, F. Borges, Antioxidant profile of dihydroxy- and trihydroxyphenolic acids--a structure-activity relationship study, *Free Radic. Res.*, vol. 40, no. 4, pp. 433–442. **2006**

[25] V.D. Kancheva, Phenolic antioxidants – radical-scavenging and chain-breaking activity: A comparative study, *European Journal of Lipid Science and Technology*, vol. 111, no. 11, pp. 1072–1089. **2009**

[26] U.J. Jung, M.-K. Lee, Y.B. Park, S.-M. Jeon, M.-S. Choi, Antihyperglycemic and antioxidant properties of caffeic acid in db/db mice, *J. Pharmacol. Exp. Ther.*, vol. 318, no. 2, pp. 476–483. **2006**

[27] M.-E. Cuvelier, H. Richard, C. Berset, Comparison of the antioxidative activity of some acid-phenols: Structure-activity relationship, *Bioscience, Biotechnology, and Biochemistry*, vol. 56, no. 2, pp. 324–325. **1992**

[28] W.-M. Wu, L. Lu, Y. Long, T. Wang, L. Liu, Q. Chen, R. Wang, Free radical scavenging and antioxidative activities of caffeic acid phenethyl ester (CAPE) and its related compounds in solution and membranes: A structure–activity insight, *Food Chemistry*, vol. 105, no. 1, pp. 107–115. **2007**

[29] J.C.J.M.D.S. Menezes, S.P. Kamat, J.A.S. Cavaleiro, A. Gaspar, J. Garrido, F. Borges, Synthesis and antioxidant activity of long chain alkyl hydroxycinnamates, *European Journal of Medicinal Chemistry*, vol. 46, no. 2, pp. 773–777. **2011**

[30] A. Gaspar, M. Martins, P. Silva, E.M. Garrido, J. Garrido, O. Firuzi, R. Miri, L. Saso, F. Borges, Dietary phenolic acids and derivatives. Evaluation of the antioxidant activity of sinapic acid and its alkyl esters, *J. Agric. Food Chem.*, vol. 58, no. 21, pp. 11273–11280. **2010**

[31] H. Kikuzaki, M. Hisamoto, K. Hirose, K. Akiyama, H. Taniguchi, Antioxidant properties of ferulic acid and its related compounds, *J. Agric. Food Chem.*, vol. 50, no. 7, pp. 2161–2168. **2002**

[32] R. Petrucci, P. Astolfi, G. Lucedio, O. Firuzi, L. Saso, G. Marrosu, A spectroelectrochemical and chemical study on oxidation of hydroxycinnamic acids in aprotic medium, *Electrochimica Acta*, vol. 52, pp. 2461–2470. **2007**

[33] J. Psotováa, J. Lasovskýb, J. Vičara, Metal-chelating properties, electrochemical behavior, scavenging and cytoprotective activities of six natural phenolics, *Biomed. Papers*, vol. 147, no. 2, pp. 147-153. **2003**

[34] C. Ekmekcioglu, J. Feyertag, W. Marktl, Cinnamic acid inhibits proliferation and modulates brush border membrane enzyme activities in Caco-2 cells, *Cancer Lett*, vol. 128, no. 2, pp. 137–144. **1998**

[35] L. Liu, W.R. Hudgins, S. Shack, M.Q. Yin, D. Samid, Cinnamic acid: a natural product with potential use in cancer intervention, *Int J Cancer*, vol. 62, no. 3, pp. 345–350. **1995**

[36] A. Nitzsche, S.V. Tokalov, H.O. Gutzeit, J. Ludwig-Müller, Chemical and biological characterization of cinnamic acid derivatives from cell cultures of lavender (Lavandula officinalis) induced by stress and jasmonic acid, *J Agric Food Chem*, vol. 52, no. 10, pp. 2915–2923. **2004**

[37] N.J. Kang, K.W. Lee, B.J. Shin, S.K. Jung, M.K. Hwang, A.M. Bode, Y.-S. Heo, H.J. Lee, Z. Dong, Caffeic acid, a phenolic phytochemical in coffee, directly inhibits Fyn kinase activity and UVB-induced COX-2 expression, *Carcinogenesis*, vol. 30, no. 2, pp. 321–330. **2009**

[38] P. De, M. Baltas, F. Bedos-Belval, Cinnamic acid derivatives as anticancer agents-a review, *Curr Med Chem*, vol. 18, no. 11, pp. 1672–1703. **2011**

[39] A.H. Banskota, T. Nagaoka, L.Y. Sumioka, Y. Tezuka, S. Awale, K. Midorikawa, K. Matsushige, S. Kadota, Antiproliferative activity of the Netherlands propolis and its active principles in cancer cell lines, *J Ethnopharmacol*, vol. 80, no. 1, pp. 67–73. **2002**
[40] K. Natarajan, S. Singh, T.R. Burke, D. Grunberger, B.B. Aggarwal, Caffeic acid phenethyl ester is a potent and specific inhibitor of activation of nuclear transcription factor NF-kappa B, *Proc Natl Acad Sci U S A*, vol. 93, no. 17, pp. 9090–9095. **1996**
[41] N.H. Nam, Y.J. You, Y. Kim, D.H. Hong, H.M. Kim, B.Z. Ahn, Syntheses of certain 3-aryl-2-propenoates and evaluation of their cytotoxicity, *Bioorg Med Chem Lett*, vol. 11, no. 9, pp. 1173–1176. **2001**
[42] B. Etzenhouser, C. Hansch, S. Kapur, C.D. Selassie, Mechanism of toxicity of esters of caffeic and dihydrocaffeic acids, *Bioorg Med Chem*, vol. 9, no. 1, pp. 199–209. **2001**
[43] C. Balachandran, N. Emi, Y. Arun, Y. Yamamoto, B. Ahilan, B. Sangeetha, V. Duraipandiyan, Y. Inaguma, A. Okamoto, S. Ignacimuthu, N.A. Al-Dhabi, P.T. Perumal, In vitro anticancer activity of methyl caffeate isolated from Solanum torvum Swartz. fruit, *Chem Biol Interact*, vol. 242, pp. 81–90. **2015**
[44] S. Apers, D. Paper, J. Bürgermeister, S. Baronikova, S. Van Dyck, G. Lemiére, A. Vlietinck, L. Pieters, Antiangiogenic activity of synthetic dihydrobenzofuran lignans, *J. Nat. Prod.*, vol. 65, no. 5, pp. 718–720. **2002**
[45] G. Basini, C. Spatafora, C. Tringali, S. Bussolati, F. Grasselli, Effects of a ferulate-derived dihydrobenzofuran neolignan on angiogenesis, steroidogenesis, and redox status in a swine cell model, *J Biomol Screen*, vol. 19, no. 9, pp. 1282–1289. **2014**
[46] S.-Y. Yin, F.-Y. Jian, Y.-H. Chen, S.-C. Chien, M.-C. Hsieh, P.-W. Hsiao, W.-H. Lee, Y.-H. Kuo, N.-S. Yang, Induction of IL-25 secretion from tumour-associated fibroblasts suppresses mammary tumour metastasis, *Nat Commun*, vol. 7, p. 11311. **2016**
[47] M.S. Barber, V.S. McConnell, B.S. DeCaux, Antimicrobial intermediates of the general phenylpropanoid and lignin specific pathways, *Phytochemistry*, vol. 54, no. 1, pp. 53–56. **2000**
[48] M. Kuhnt, A. Pröbstle, H. Rimpler, R. Bauer, M. Heinrich, Biological and pharmacological activities and further constituents of Hyptis verticillata, *Planta Med*, vol. 61, no. 3, pp. 227–232. **1995**
[49] K. Tonari, K. Mitsui, K. Yonemoto, Structure and antibacterial activity of cinnamic acid related compounds, *Journal of Oleo Science*, vol. 51, no. 4, pp. 271–273. **2002**
[50] S. Tewtrakul, H. Miyashiro, N. Nakamura, M. Hattori, T. Kawahata, T. Otake, T. Yoshinaga, T. Fujiwara, T. Supavita, S. Yuenyongsawad, P. Rattanasuwon, S. Dej-Adisai., HIV-1 integrase inhibitory substances from Coleus parvifolius, *Phytother Res*, vol. 17, no. 3, pp. 232–239. **2003**
[51] P.A. Turhanen, J. Leppänen, J.J. Vepsäläinen, Green and efficient esterification method using dried Dowex H+/NaI approach, *ACS Omega*, vol. 4, no. 5, pp. 8974–8984. **2019**
[52] I. Pastan, M.M. Gottesman, K. Ueda, E. Lovelace, A.V. Rutherford, M.C. Willingham, A retrovirus carrying an MDR1 cDNA confers multidrug resistance and polarized expression of P-glycoprotein in MDCK cells, *Proc. Natl. Acad. Sci. U.S.A.*, vol. 85, no. 12, pp. 4486–4490. **1988**
[53] A.D. Latif, T. Gonda, M. Vágvölgyi, N. Kúsz, Á. Kulmány, I. Ocsovszki, Z. Zomborszki, I. Zupkó, A. Hunyadi, Synthesis and in vitro antitumor activity of naringenin oxime and oxime ether derivatives, *Int J Mol Sci*, vol. 20, no. 9, p. 2184. **2019**
[54] H.-C. Wang, A. Y.-L. Lee, W.-C. Chou, C.-C. Wu, C.-N. Tseng, K. Y.-T. Liu, W.-L. Lin, F.-R. Chang, D.-W. Chuang, A. Hunyadi, Y.-C. Wu, Inhibition of ATR-dependent signaling by protoapigenone and its derivative sensitizes cancer cells to interstrand cross-link–generating agents in vitro and in vivo', *Mol Cancer Ther*, vol. 11, no. 7, pp. 1443–1453. **2012**
[55] S. Mathew, T. E. Abraham, In vitro antioxidant activity and scavenging effects of Cinnamomum verum leaf extract assayed by different methodologies, *Food Chem. Toxicol.*, vol. 44, no. 2, pp. 198–206. **2006**
[56] B. Tadolini, L. Cabrini, The influence of pH on OH scavenger inhibition of damage to deoxyribose by Fenton reaction, *Mol Cell Biochem*, vol. 94, no. 2, pp. 97–104. **1990**
[57] H. Kim, J. Ralph, F. Lu, S.A. Ralph, A.M. Boudet, J.J. MacKay, R.R. Sederoff, T. Ito, S. Kawai, H. Ohashi, T. Higuchi, NMR analysis of lignins in CAD-deficient plants. Part 1. Incorporation of hydroxycinnamaldehydes and hydroxybenzaldehydes into lignins, *Org Biomol Chem*, vol. 1, no. 2, pp. 268–281. **2003**

[58] M.A.K. Zarchi, F. Rahmani, Regioselective and green synthesis of nitro aromatic compounds using polymer-supported sodium nitrite/KHSO4, *Journal of Applied Polymer Science*, vol. 120, no. 5, pp. 2830–2834. **2011**
[59] B. Schmidt, F. Hölter, R. Berger, S. Jessel, Mizoroki–Heck reactions with 4-Phenoldiazonium salts, *Advanced Synthesis & Catalysis*, vol. 352, no. 14–15, pp. 2463–2473. **2010**
[60] K. Matsuki, M. Sobukawa, A. Kawai, H. Inoue, M. Takeda, Asymmetric reduction of aromatic ketones. II. An enantioselective synthesis of Methyl (2R, 3S)-3-(4-Methoxyphenyl)glycidate, *Chemical & Pharmaceutical Bulletin*, vol. 41, no. 4, pp. 643–648. **1993**
[61] P.B.D. de la Mare, M.A. Wilson, M.J. Rosser, The kinetics and mechanisms of additions to olefinic substances. Part XI. Stereochemistry of addition of chlorine acetate and of chlorine to some unsaturated compounds, *J. Chem. Soc., Perkin Trans. 2*, no. 10, pp. 1480–1490. **1973**
[62] H. Inoue, K. Matsuki, T. Oh-Ishi, A new enantioselective synthesis of (2R, 3S)-3-(4-Methoxyphenyl)glycidic ester via the enzymatic hydrolysis of erythro-N-Acetyl-β-(4-methoxyphenyl)serine, *Chemical & Pharmaceutical Bulletin*, vol. 41, no. 9, pp. 1521–1523. **1993**
[63] O. Cabon, D. Buisson, M. Larcheveque, R. Azerad, The microbial reduction of 2-chloro-3-oxoesters, *Tetrahedron: Asymmetry*, vol. 6, no. 9, pp. 2199–2210. **1995**
[64] K. Matsumoto, H. Takahashi, Y. Miyake, Y. Fukuyama, Convenient syntheses of neurotrophic americanol A and isoamericanol A by HRP catalyzed oxidative coupling of caffeic acid, *Tetrahedron Letters*, vol. 40, no. 16, pp. 3185–3186. **1999**
[65] T.-C. Chou, Theoretical basis, experimental design, and computerized simulation of synergism and antagonism in drug combination studies, *Pharmacol Rev*, vol. 58, no. 3, pp. 621–681. **2006**
[66] G.T. Balogh, K. Vukics, A. Könczöl, A. Kis-Varga, A. Gere, J. Fischer, Nitrone derivatives of trolox as neuroprotective agents, *Bioorg Med Chem Lett*, vol. 15, no. 12, pp. 3012–3015. **2005**
[67] A. Urbaniak, M. Molski, M. Szeląg, Quantum-chemical calculations of the antioxidant properties of trans-p-coumaric Acid and trans-sinapinic acid, *Computational Methods in Science and Technology*, vol. 18, no. 2, pp. 117-128. **2012**
[68] T. H. Chuang, H. H. Chan, T. S. Wu, C. F. Li, Chemical constituents and biological studies of the leaves of grevillea robusta, *Molecules*, vol. 16, no. 11, pp. 9331–9339. **2011**
[69] Atta-ur-Rahman, M. Shabbir, S. Ziauddin Sultani, A. Jabbar, M. Iqbal Choudhary, Cinnamates and coumarins from the leaves of Murraya paniculata, *Phytochemistry*, vol. 44, no. 4, pp. 683–685. **1997**
[70] F.-X. Felpin, Oxidation of 4-arylphenol trimethylsilyl ethers to p-arylquinols using hypervalent iodine(III) reagents, *Tetrahedron Letters*, vol. 3, no. 48, pp. 409–412. **2007**
[71] H. Hamamoto, G. Anilkumar, H. Tohma, Y. Kita, A novel and useful oxidative intramolecular coupling reaction of phenol ether derivatives on treatment with a combination of hypervalent iodine(III) reagent and heteropoly acid, *Chemistry – A European Journal*, vol. 8, no. 23, pp. 5377–5383. **2002**
[72] B. Dankó, A. Martins, D.-W. Chuang, H.-C. Wang, L. Amaral, J. Molnár, F.-R. Chang, Y.-C. Wu, A. Hunyadi, In vitro cytotoxic activity of novel protoflavone analogs - selectivity towards a multidrug resistant cancer cell line, *Anticancer Res*, vol. 32, no. 7, pp. 2863–2869. **2012**
[73] B. Dankó, Sz. Tóth, A. Martins, M. Vágvölgyi, N. Kúsz, J. Molnár, F.-R. Chang, Y.-C. Wu, G. Szakács, A. Hunyadi, Synthesis and SAR study of anticancer protoflavone derivatives: investigation of cytotoxicity and interaction with ABCB1 and ABCG2 multidrug efflux transporters, *ChemMedChem*, vol. 12, no. 11, pp. 850–859. **2017**
[74] B. Ou, M. Hampsch-Woodill, R.L. Prior, Development and validation of an improved oxygen radical absorbance capacity assay using fluorescein as the fluorescent probe, *J. Agric. Food Chem.*, vol. 49, no. 10, pp. 4619–4626. **2001**
[75] A. Denicola, J.M. Souza, and R. Radi, Diffusion of peroxynitrite across erythrocyte membranes, *Proc Natl Acad Sci U S A*, vol. 95, no. 7, pp. 3566–3571. **1998**
[76] K.M. Robinson and J.S. Beckman, Synthesis of peroxynitrite from nitrite and hydrogen peroxide, *Meth. Enzymol.*, vol. 396, pp. 207–214. **2005**
[77] H. Rubbo, R. Radi, Protein and lipid nitration: role in redox signaling and injury, *Biochim Biophys Acta*, vol. 1780, no. 11, pp. 1318–1324. **2008**
[78] P. Pacher, J.S. Beckman, L. Liaudet, Nitric oxide and peroxynitrite in health and disease, *Physiol Rev*, vol. 87, no. 1, pp. 315–424. **2007**

[79] R. Radi, Oxygen radicals, nitric oxide, and peroxynitrite: Redox pathways in molecular medicine, *Proc Natl Acad Sci U S A*, vol. 115, no. 23, pp. 5839–5848. **2018**
[80] G. Szakács, M.D. Hall, M.M. Gottesman, A. Boumendjel, R. Kachadourian, B.J. Day, H. Baubichon-Cortay, A. Di Pietro, Targeting the Achilles heel of multidrug-resistant cancer by exploiting the fitness cost of resistance, *Chem. Rev.*, vol. 114, no. 11, pp. 5753–5774. **2014**
[81] K. Robinson, V. Tiriveedhi, Perplexing role of P-glycoprotein in umor microenvironment, *Front. Oncol.*, vol. 10., no. 265. **2020**
[82] L.J. Kuo, L.-X. Yang, Gamma-H2AX - a novel biomarker for DNA double-strand breaks, *In Vivo*, vol. 22, no. 3, pp. 305–309. **2008**
[83] T. Stankovic, B. Dankó, A. Martins, M. Dragoj, S. Stojkovic, A. Isakovic, H.-C. Wang, Y.-C. Wu, A. Hunyadi, M. Pesic, Lower antioxidative capacity of multidrug-resistant cancer cells confers collateral sensitivity to protoflavone derivatives, *Cancer Chemotherapy and Pharmacology*, vol. 76, no. 3, pp. 555-565. **2015**
[84] M.B. Kastan, J. Bartek, Cell-cycle checkpoints and cancer, *Nature*, vol. 432, no. 7015, pp. 316–323. **2004**
[85] C.C. Chen, R.D. Kennedy, S.Sidi, A.T. Look, A. D'Andrea, CHK1 inhibition as a strategy for targeting Fanconi Anemia (FA) DNA repair pathway deficient tumors, *Mol Cancer*, vol. 8, p. 24. **2009**
[86] K.A. Cole, J. Huggins, M. Laquaglia, C.E. Hulderman, M.R. Russell, K. Bosse, S.J. Diskin, E.F. Attiyeh, R. Sennett, G. Norris, M. Laudenslager, A.C. Wood, P.A. Mayes, J. Jagannathan, C. Winter, Y.P. Mosse, J.M. Maris, RNAi screen of the protein kinome identifies checkpoint kinase 1 (CHK1) as a therapeutic target in neuroblastoma, *Proc Natl Acad Sci U S A*, vol. 108, no. 8, pp. 3336–3341. **2011**
[87] K. Brooks, V. Oakes, B. Edwards, M. Ranall, P. Leo, S. Pavey, A. Pinder, H. Beamish, P. Mukhopadhyay, D. Lambie, B. Gabrielli, A potent Chk1 inhibitor is selectively cytotoxic in melanomas with high levels of replicative stress, *Oncogene*, vol. 32, no. 6, pp. 788–796. **2013**
[88] B. Halliwell, Cell culture, oxidative stress, and antioxidants: avoiding pitfalls, *Biomed J*, vol. 37, no. 3, pp. 99–105. **2014**
[89] D. Figueroa, M. Asaduzzaman, F. Young, Real time monitoring and quantification of reactive oxygen species in breast cancer cell line MCF-7 by 2',7'-dichlorofluorescin diacetate (DCFDA) assay, *J Pharmacol Toxicol Methods*, vol. 94, no. Pt 1, pp. 26–33. **2018**
[90] Y.S. Kwon, C.M. Kim, Antioxidant constituents from the stem of Sorghum bicolor, *Arch Pharm Res*, vol. 26, no. 7, pp. 535–539. **2003**
[91] I. Kiliç, Y. Yeşiloğlu, Spectroscopic studies on the antioxidant activity of p-coumaric acid, *Spectrochim Acta A Mol Biomol Spectrosc*, vol. 115, pp. 719–724. **2013**

ACKNOWLEDGEMENTS

Firstly, I would like to express my sincere gratitude to my supervisor, Dr. Attila Hunyadi, for the continuous professional support, the motivation, and for his patience. I would also like to give a special thanks to my co-supervisor, Prof. Fang-Rong Chang for directing and supporting my PhD work during my 6-month exchange studies at the Graduate Institute of Natural Products, Kaohsiung Medical University, Kaohsiung, Taiwan.

I would like to thank Prof. Dr. Judit Hohmann, Head of the Institute of Pharmacognosy, for the possibility to study in her department.

I am thankful to Dr. Zoltán Béni for the NMR investigations and Dr. Miklós Dékány for the mass spectrometry measurements.

My sincere thanks go to Dr. Ana Martins for testing the oxidized metabolites for their antitumor activity. I would like to thank to Dr. Milica Pešić and Dr. Sonja Stojković Burić for performing the cell death analysis and investigating DNA damage by flow cytometry. I am also thankful to Prof. Hui-Chun Wang and Dr. Ching-Ying Kuo for performing the experiments for the DNA damage response study. I would like to thank Prof. István Zupkó and Dr. Ahmed Dhahir Latif for cell viability testing on gynecological cancer cell lines and for the comparative cytotoxicity testing with or without the presence of *t*-BHP-induced oxidative stress.

I owe special thanks to Prof. Patrick Trouillas and Dr. Florent Di Meo for the *in silico* calculations.

I am grateful to Dr. György Tibor Balogh, who provided me an opportunity to join his team at the Compound Profiling Laboratory at the Richter Gedeon Plc., and supported me in carrying out the continuous-flow reactions and let me acquire knowledge in LC-MS measurements. I would like to thank to Sándor Lévai, who helped me in the preparative HPLC purifications at Gedeon Richter Plc.

I would like to give a special thanks to Ibolya Hevérné Herke for the lot of help she provided during my lab work, for her scientific advices and encouragement.

I am also thankful to all my colleagues in the Institute of Pharmacognosy, especially my fellow labmates for their support and for the time we spent together.

I would like to thank to my family, my fiancé and friends for supporting me all the time during my PhD study.

This work was supported by the National Research, Development and Innovation Office, Hungary (NKFIH; K119770), the Ministry of Human Capacities, Hungary grant 20391-3/2018/FEKUSTRAT, and by a bilateral mobility grant from the Hungarian Academy of Sciences and the Ministry of Science and Technology, Taiwan (MOST 107-2911-I-037-502).